late-onset cortical cerebellar atrophy (LCCA) and 2 patients with spinocerebellar ataxia (SCA) 6, diagnosed by genetic analysis of the SCA mutations. The other three patients had a family history of cerebellar ataxia with a dominant pattern of inheritance. Although they were diagnosed with autosomal-dominant inherited cerebellar ataxia (ADCA), the type of ADCA could not be determined because the patients refused genetic analysis of the SCA mutations. All patients received a neurologic examination by a neurologist and a diagnostic evaluation that included a head-up tilt test, routine laboratory tests including the complete blood count, urine components, blood biochemistry, thyroid function, vitamin E levels, and tumor markers. We performed neurophysiologic testing, including a peripheral nerve conduction study, heart rate variability analysis, electroencephalogram, brain magnetic resonance imaging (MRI), and SPECT. In addition, a lumbar puncture was performed in all patients to exclude the possibility of an infectious, immunologic, or paraneoplastic cause. Because there are no standardized criteria for diagnosing idiopathic LCCA, a diagnosis of LCCA in the present study was made according to the following criteria: 1) age onset <30 years; 2) pure cerebellar syndrome; 3) absence of severe abnormalities on nerve conduction studies; 4) no abnormalities on cystometry, a head-up tilt test and coefficient of variation of the R–R interval; 5) no family history of an ataxia syndrome; 6) absence of a potential toxic cause that could explain the ataxia (alcoholism, anticonvulsant drugs); 7) slowly progressive disease course; 8) exclusion of cerebellar syndromes due to other causes, such as an autoimmune-mediated cerebellar ataxia, paraneoplastic ataxia, alcoholic ataxia, and ataxia with hypothyroidism. TRH (2 mg/day) was administered intravenously daily for 14 days. Clinical evaluation was recorded before and after treatment using the International Cooperative Ataxia Rating Scale (ICARS) [15]. The same person assessed the ICARS for each patient, but could not be blinded to the treatment because healthy control subjects were not included in the study. The ICARS score was expressed as mean value ± standard deviation and compared between before and after TRH therapy.

2.2. Brain SPECT imaging

SPECT was performed in all subjects before and after TRH therapy. Patients were asked to maintain a comfortable supine position with eyes closed in quiet surroundings. After intravenous injection of 99mTc ethylcysteinate dimer (600 MBq, FUJIFILM RI Pharma Co., Ltd. Japan), its passage from the heart to the brain was monitored using a rectangular large field gamma camera (E. Cam Signature, Toshiba Medical, Japan). Ten minutes after the angiography, SPECT images were obtained using a rotating, dual-head gamma camera. Data were acquired as a sequence of 120 frames at a rate of 1 frame per second with a 128 × 128 matrix. All SPECT images were reconstructed using a ramp-filtered back-projection and then three-dimensionally smoothed with a Butterworth filter. The reconstructed images were corrected for gamma ray attenuation using the Chang method. For rCBF quantification, the noninvasive Patlak plot method [16,17] was used on a 99mTc ethylcysteinate dimer cerebral blood flow perfusion SPECT. Quantitative flow-mapping images were obtained from the qualitative perfusion images using Patlak plot graphical analysis and Lassen's correction, as previously reported [13,18,19]. The rCBF in each ROI was calculated using the 3DSRT software, which is a fully automated ROI technique developed by Takeuchi et al. [12]. The blood flow in each ROI was quantified as the value in milliliters per 100 g/min. These ROIs were categorized into 12 segments; the callosomarginal, precentral, central, parietal, angular, temporal, posterior cerebral, pericallosal, lenticular nucleus, thalamus, hippocampus, and cerebellum segments in the template, and the rCBF was expressed as the mean value ± standard deviation bilaterally for each segment [12,13]. The mean rCBF in all segments was compared between before and after TRH therapy. We also used an easy *Z*-score imaging system (eZIS) program to supplement the diagnosis and to detect a statistically significant decrease in blood perfusion. A *Z*-score map for each SPECT image was extracted from the comparison with the mean and SD of SPECT images of age-matched normal controls that had been incorporated into the eZIS program as a normal control database. A voxel-by-voxel *Z* score analysis was performed after voxel normalization to global means or cerebellar values; Z-score = ([control mean] − [individual value] / (control SD). These *Z*-score maps were displayed by overlaying them on tomographic sections and projecting the averaged *Z*-score of a 14 mm thickness-to-surface rendering of the anatomically standardized magnetic resonance (MR) imaging template [10,11].

2.3. Statistical analysis

The differences in the rCBF and ICARS before and after TRH therapy were analyzed using the paired *t*-test. The correlations between the improved ICARS scores and the disease duration as well as the ICARS scores at baseline were evaluated by regression analysis. In addition, the correlations between the increased rCBF in the cerebellum and the disease duration, and the ICARS scores at baseline and the ICARS scores after treatment were evaluated by regression analysis. A *p* value of less than 0.05 was considered to be statistically significant.

3. Results

The clinical characteristics of all the patients are shown in Table 1. The mean age was 60.8 ± 6.7 years and the mean disease duration at the time of TRH therapy was 9.6 ± 7.9 years. Neurologic examination revealed limb ataxia, truncal ataxia, ataxic gait, and/or gaze-evoked nystagmus without parkinsonism, autonomic, and pyramidal signs characteristic of the cerebellar form of SCD. The baseline mean ICARS

Table 1
Clinical presentation of patients with spinocerebellar ataxia.

	Sex	Age (y)	Duration (y)	Diagnosis	ICARS		mCBF		Cerebellar rCBF	
					Before	After	Before	After	Before	After
Patient 1	M	55	2	LCCA	35	35	37.8	42.0	38.0	41.5
Patient 2	M	54	13	LCCA	53	53	40.6	40.1	43.5	43.1
Patient 3	F	69	8	LCCA	30	25	37.2	37.2	32.1	35.3
Patient 4	F	67	1	LCCA	17	10	47.6	49.0	47.3	53.0
Patient 5	M	63	3	LCCA	28	19	40.7	38.1	36.1	34.5
Patient 6	F	52	6	SCA6	29	29	45.4	44.7	45.5	45.4
Patient 7	M	59	17	SCA6	69	69	43.0	43.3	35.3	35.4
Patient 8	M	54	8	ADCA	36	30	40.0	40.5	37.4	40.8
Patient 9	F	66	27	ADCA	48	50	43.3	43.2	34.8	37.9
Patient 10	M	69	11	ADCA	44	41	39.2	42.6	45.4	46.9

M: Male. F: Female. Duration: Disease duration. y: Year. ICARS: International Cooperative Ataxia Rating Scale. mCBF: Mean value of the cerebral blood flow in the bilateral cerebral hemisphere before and after therapy (milliliters per 100 g/min). Cerebellar rCBF: Mean value of the cerebral blood flow in the bilateral cerebellum before and after therapy (milliliters per 100 g/min).

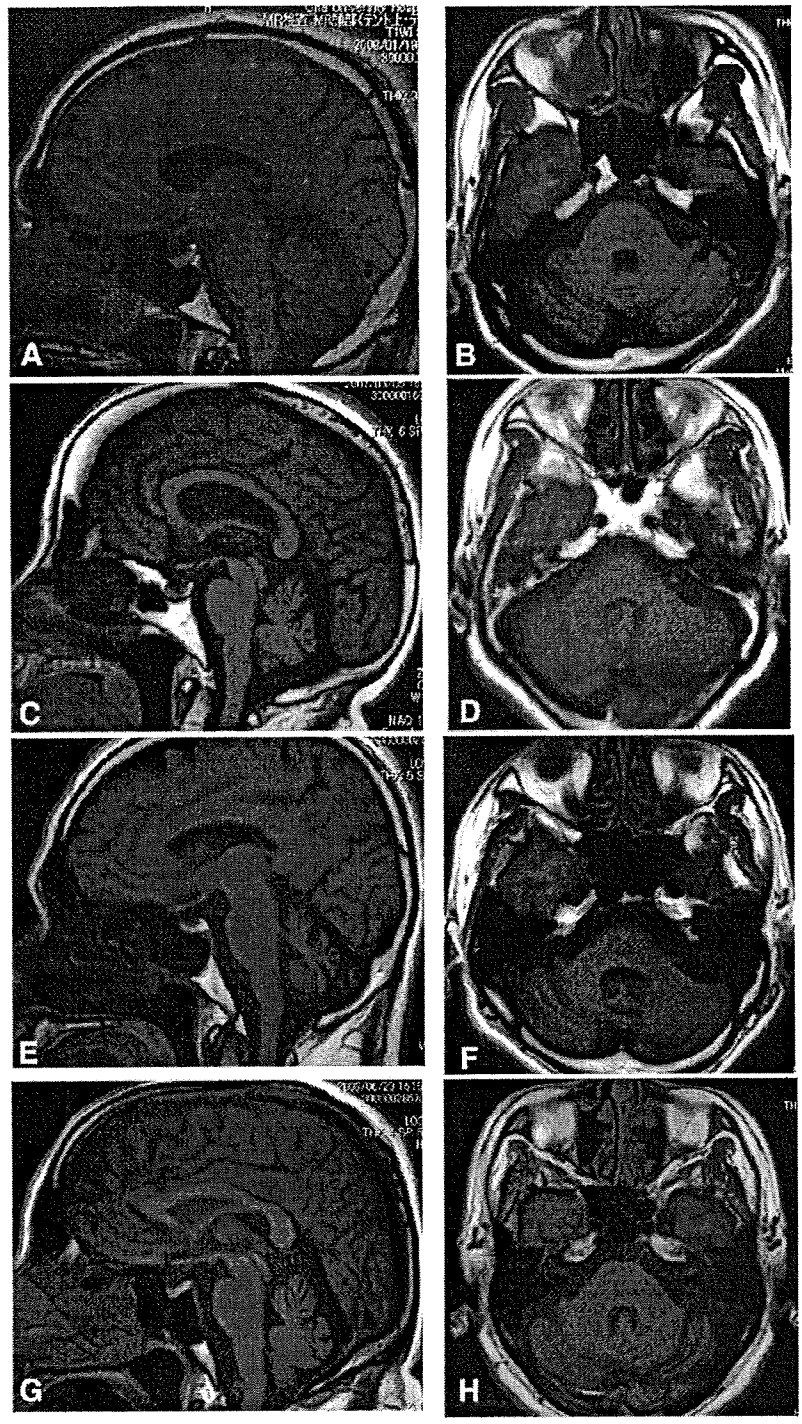

Fig. 1. T1-weighted MR images (sagittal and axial images) in patients with LCCA (patients 1 and 3), SCA-6 (patient 7), and ADCA (patient 10). Cerebellar atrophy without brainstem involvement was mild in patient 3 (C,D) and moderate in patients 1 (A,B), 7 (E,F), and 10 (G,H).

value was 38.9 ± 14.9 (range, 17–69), indicating high variability in the disease severity between patients. The mean whole brain CBF value did not change after TRH therapy (before: 41.4 ± 3.3, after: 42.0 ± 3.4 ml/100 g brain/min). MRI demonstrated various degrees of brain atrophy in the cerebellar hemisphere and vermis without brainstem involvement in all patients (Fig. 1). The eZIS analysis detected a relative decrease in cerebellar rCBF in all patients compared with the normal values from the control data (Fig. 2). There was no relative rCBF reduction in any region of the cerebrum or brainstem. The spatial distribution and degree of rCBF reduction in the cerebellum varied between patients, and corresponded to the cerebellar atrophy on MR images. Following TRH therapy, the ICARS score decreased in 5 patients, increased in 1 patient, and did not change in 4 patients. The mean ICARS score significantly decreased from 38.9 ± 14.9 to 36.1 ± 17.5 (Fig. 3; $p = 0.03$, paired t test). The ICARS scores after TRH therapy did not significantly differ between patients with LCCA and ADCA, including SCA 6. The improved ICARS score tended to correlate inversely with disease

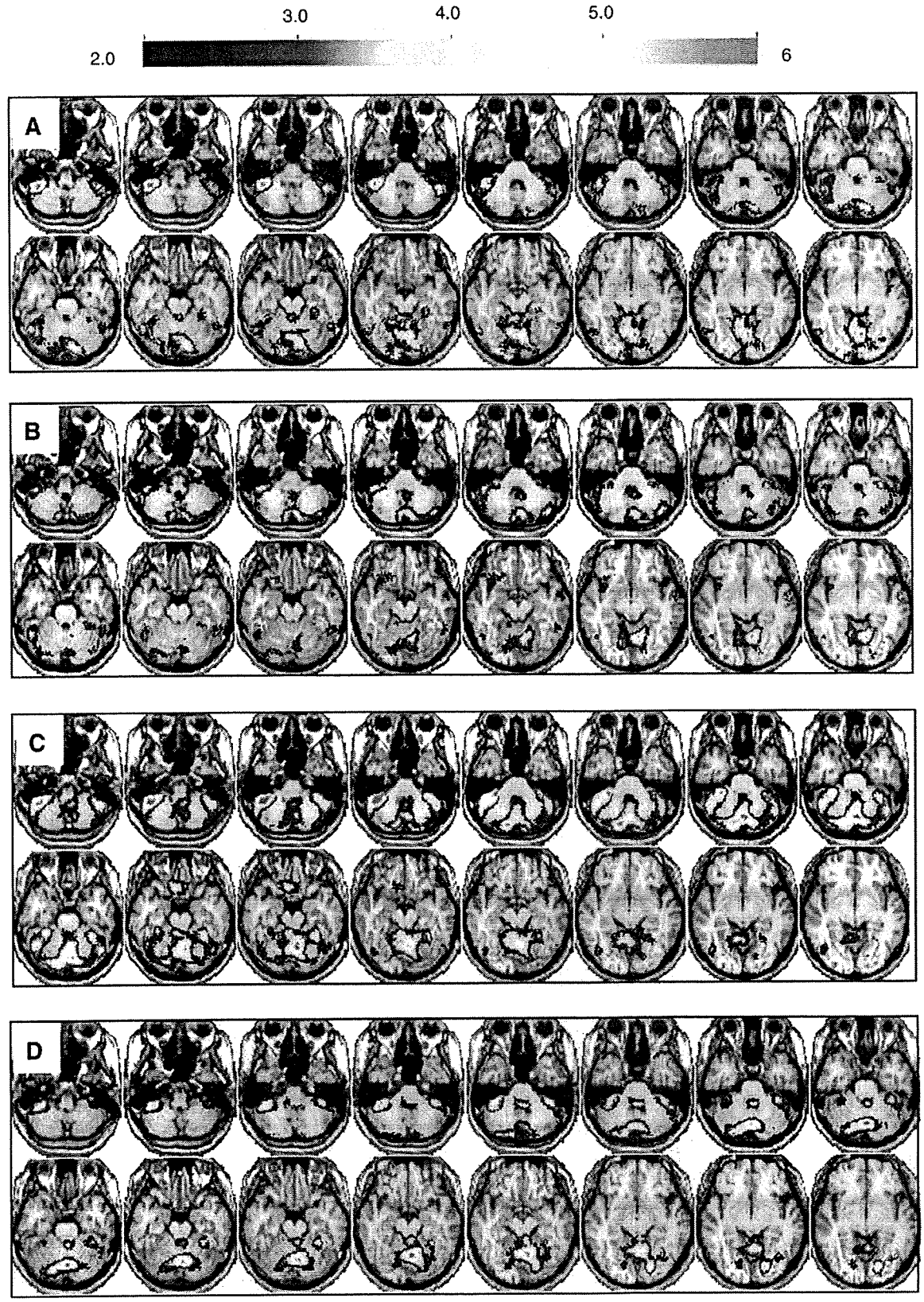

Fig. 2. eZIS images in (axial view) patients with LCCA (patient 1 and 3), SCA-6 (patient 7), and ADCA (patient 10). The color images represent the statistical significance (Z-score) of the decrease in rCBF. The relative rCBF reduction in the cerebellum was significant, but mild, in patient 3 (B) and moderate in patients 1 (A), 7 (C), and 10 (D). The relative rCBF reduction was detected predominantly in the vermis in patients 1 (A), 3 (B), and 10 (D). The relative rCBF reduction was detected predominantly in the cerebellar hemispheres and vermis in patient 7 (C).

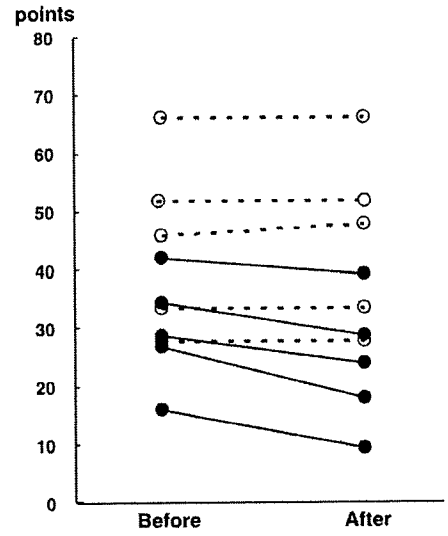

Fig. 3. International Cooperative Ataxia Rating Scale (ICARS) score before and after TRH therapy. ICARS score decreased in 5 patients, increased in 1 patient, and did not change in 4 patients. The mean values of ICARS score were significantly decreased ($p=0.03$, paired t test). ●; patient with decreased ICARS score, ○; patient with stable or increased ICARS score.

duration and baseline ICARS score, but this was not statistically significant ($p=0.051$ and $p=0.059$, regression analysis).

The cerebellar rCBF increased in 7 patients and decreased in 1 patient following TRH therapy. In addition, the cerebellar rCBF did not change in the other 2 patients (Fig. 4). Increased cerebellar rCBF was observed in 7 patients, including 3 patients with LCCA and 4 patients with ADCA. There were no significant differences in the increased cerebellar rCBF between patients with LCCA and ADCA including SCA 6. Increased cerebellar rCBF did not correlate with disease duration, baseline ICARS scores, or improved ICARS scores ($p=0.72$, $p=0.24$, and $p=0.80$, respectively; regression analysis). In 4 of the 5 patients with improved ICARS scores, however, cerebellar rCBF increased after TRH therapy. In addition, 3 of the remaining 5 patients without

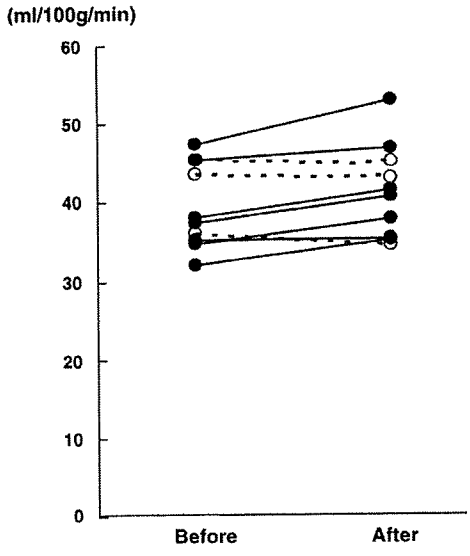

Fig. 4. Cerebellar blood flow before and after TRH therapy calculated using 3DSRT. Cerebellar rCBF increased in 7 patients and decreased in 1 patient. Cerebellar rCBF did not change in 2 patients. The mean values of cerebellar rCBF were significantly increased ($p=0.03$, paired t test). ●; patient with increased cerebellar rCBF, ○; patient with stable or decreased cerebellar rCBF.

Table 2
Regional cerebral blood flow (rCBF) before and after TRH therapy calculated using 3DSRT.

Region	rCBF (before)	rCBF (after)	p value
Callosomarginal	40.87 ± 4.59	42.98 ± 9.10	0.037*
Precentral	40.84 ± 3.76	42.67 ± 8.89	0.081
Central	37.31 ± 4.04	38.74 ± 8.08	0.209
Parietal	37.11 ± 3.39	38.65 ± 7.99	0.104
Angular	38.68 ± 3.04	40.52 ± 8.30	0.052
Temporal	36.26 ± 2.72	37.34 ± 7.80	0.146
Occipital	38.00 ± 2.86	39.36 ± 8.24	0.095
Pericallosal	41.14 ± 4.31	43.02 ± 9.00	0.088
Lenticular nucleus	42.57 ± 4.79	43.51 ± 9.70	0.536
Thalamus	42.77 ± 4.79	43.22 ± 9.67	0.730
Hippocampus	31.11 ± 3.75	31.79 ± 6.90	0.420
Cerebellum	39.54 ± 5.38	41.39 ± 9.18	0.030*

The rCBF is expressed as mean ± SD (milliliter per 100 g/min). rCBF: Mean value of regional cerebral blood flow bilaterally in each segment.
* $p<0.05$.

improved ICARS scores, had increased cerebellar rCBF. A comparison of the mean rCBF in each segment both before and after treatment is shown in Table 2. Statistical analysis revealed a significant increase in the rCBF in the callosomarginal segment and cerebellum ($p=0.037$ and $p=0.030$, paired t test).

4. Discussion

The results of the present study indicated an increase in cerebellar rCBF following intravenous administration of TRH at a dose of 2 mg/day for 14 days in patients with the cerebellar form of SCD. Quantitative analyses of the rCBF using 3DSRT before and after TRH therapy were performed. On the MR images, all patients with pure cerebellar ataxia showed cerebellar atrophy without brainstem and cerebral involvement. The eZIS analysis revealed a relative decrease of rCBF in the cerebellum without brainstem involvement in all patients compared to the control data, consistent with the results of previous studies on eZIS analysis of the cerebellar form of SCD [20,21].

TRH therapy might improve cerebellar ataxia in SCD, but the lack of a significant effect based on clinical observations has also been reported [22]. These conflicting results are likely due to difficulties in quantitatively assessing the efficacy based on a bedside evaluation. The ICARS is very useful for pharmacologic assessment of cerebellar ataxia, but the score may be affected by the skill and subjective assessment of the observer or the patient's condition. Therefore, a more objective and quantitative method is necessary to elucidate the efficacy of TRH therapy. Although manual quantitative measurements of rCBF have been used to assess the effects of TRH, the reproducibility and objectivity of the results are problematic [3,9]. In the present study, the rCBF in each ROI was measured automatically and objectively using a fully automated ROI technique, 3DSRT. The results revealed that THR therapy significantly improved the ICARS score and significantly increased rCBF in the callosomarginal segment and cerebellum. The improved ICARS scores tended to be higher in patients with shorter disease duration and milder disability than in those with longer disease duration and more severe disability. These findings reconfirm that TRH therapy is a worthy therapeutic modality for patients with SCD in the early clinical stage. Although our findings do not indicate a significant correlation between the increased cerebellar rCBF and improved ICARS scores, likely due to the small number of patients, 4 of the 5 patients with improved ICARS scores had increased cerebellar rCBF after TRH therapy. We suggest that 3DSRT may be a useful tool for evaluating of the efficacy of TRH therapy for increasing cerebral blood flow and may help to distinguish between TRH therapy responders and non-responders.

The mechanism underlying the efficacy of TRH therapy in patients with SCD remains unclear. Following intravenous TRH administration

for 14 days, rCBF was significantly increased in the callosomarginal segment and cerebellum, despite the fact that there was no significant change in the whole brain CBF. Although TRH and TRH receptors are widely distributed throughout the central nervous system [23,24], increased rCBF was not observed in other brain regions. Previous human studies on TRH therapy reported an increased CBF in the cerebrum in cases of viral encephalopathy, but no significant changes in rCBF were observed in healthy controls [25]. In an animal study of TRH therapy, there was an increase in the cortical CBF in anesthetized rabbits, whereas no changes in CBF were observed in awake control rabbits [26]. These results suggest that TRH may be an effective treatment in pathologic conditions and may increase rCBF only in affected regions. Therefore, we propose that the effects of TRH may be due to increased rCBF in the cerebellum, the region of degeneration in SCD. Moreover, although our patients did not show clinical and radiologic findings of frontal lobe involvement, rCBF was increased in the callosomarginal segment. One possible explanation for this finding might be a remote effect of the improved cerebellar function because there is an extensive anatomic connection between the cerebellum and the frontal and parietal lobes [27].

The mechanism of increased rCBF may be related with the cerebral vasodilatation, which is mediated by the cholinergic system and prostaglandin [28]. TRH may also activate an intrinsic cholinergic vasodilative system (in the submesencephalic brainstem, including the fastigial nucleus), which increases CBF [29–31]. Therefore, we suggest that TRH therapy increases the rCBF in the cerebellum, possibly through activation of the cholinergic vasodilative system.

There are several limitations to the present study. The number of patients with SCD was relatively small and we were unable to measure the effects of TRH on blood perfusion in healthy subjects for a control group. Also, the ICARS was assessed by the same person who was not blinded to the treatment. Further studies with bigger samples, including normal control groups, are needed to confirm our results.

In conclusion, we suggest that TRH therapy increases cerebellar rCBF and may be worthy of a trial therapeutic modality for patients with the cerebellar form of SCD. The beneficial effects of TRH may be due to the increased cerebellar rCBF or the increase in the cerebellar rCBF may be only a secondary effect. 3DSRT may be a useful tool for evaluating the efficacy of TRH therapy for increasing cerebral blood flow.

References

[1] Morley JE. Extrahypothalamic thyrotropin releasing hormone (TRH) — its distribution and its functions. Life Sci 1979;25:1539–50.
[2] Tanaka K, Ogawa N, Asanuma M, Kondo Y. Thyrotropin releasing hormone prevents abnormalities of cortical acetylcholine and monoamines in mice following head injury. Regul Pept 1997;18:173–8.
[3] Yoshinari S, Hamano S, Tanaka M, Minamitani M. Alteration of regional cerebral blood flow to thyrotropin-releasing hormone therapy in acute encephalitis and encephalopathy during childhood. Eur J Paediatr Neurol 2006;10:124–8.
[4] Nakamura R, Fujita M. Effect of thyrotropin-releasing hormone (TRH) on motor performance of hemiparetic stroke patients. Tohoku J Exp Med 1990;160:141–3.
[5] Luo L, Yano N, Mao Q, Jackson IM, Stopa EG. Thyrotropin releasing hormone (TRH) in the hippocampus of Alzheimer patients. J Alzheimers Dis 2002;4:97–103.
[6] Takeuchi Y, Miyanomae Y, Komatsu H, Oomizono Y, Nishimura A, Okano S, et al. Efficacy of thyrotropin-releasing hormone in the treatment of spinal muscular atrophy. J Child Neurol 1994;9:287–9.
[7] Sobue I, Yamamoto H, Konagaya M, Iida M, Takayanagi T. Effect of thyrotropin-releasing hormone on ataxia of spinocerebellar degeneration. Lancet 1980;1:418–9.
[8] Sobue I, Takayanagi T, Nakanishi T, Tsubaki T, Uono M, Kinoshita M, et al. Controlled trial of thyrotropin releasing hormone tartrate in ataxia of spinocerebellar degenerations. J Neurol Sci 1983;61:235–48.
[9] Izumi Y, Fukuuchi Y, Ishihara N, Imai A, Komatsumoto S. Effect of thyrotropin-releasing hormone (TRH) on cerebral blood flow in spinocerebellar degeneration and cerebrovascular disease. Tokai J Exp Clin Med 1995;20:203–8.
[10] Waragai M, Yamada T, Matsuda H. Evaluation of brain perfusion SPECT using an easy Z-score imaging system (eZIS) as an adjunct to early-diagnosis of neurodegenerative diseases. J Neurol Sci 2007;260(1–2):57–64.
[11] Matsuda H, Mizumura S, Nagao T, Ota T, Iizuka T, Nemoto K, et al. Automated discrimination between very early Alzheimer disease and controls using an easy Z-score imaging system for multicenter brain perfusion single-photon emission tomography. AJNR Am J Neuroradiol 2007;28:731–6.
[12] Takeuchi R, Sengoku T, Matsumura K. Usefulness of fully automated constant ROI analysis software for the brain: 3DSRT and FineSRT. Radiat Med 2006;24:538–44.
[13] Tateno M, Utsumi K, Kobayashi S, Takahashi A, Saitoh M, Morii H, et al. Usefulness of a blood flow analyzing program 3DSRT to detect occipital hypoperfusion in dementia with Lewy bodies. Prog Neuropsychopharmacol Biol Psychiatry 2008;32:1206–9.
[14] Waragai M, Ogawara K, Takaya Y, Hayashi M. Efficacy of TRH-T for spinocerebellar degeneration — the relation between clinical features and effect of TRH therapy. Clin Neurol 1997;37:587–94.
[15] Trouillas P, Takayanagi T, Hallett M, Currier RD, Subramony SH, Wessel K, et al. International Cooperative Ataxia Rating Scale for pharmacological assessment of the cerebellar syndrome. The Ataxia Neuropharmacology Committee of the World Federation of Neurology. J Neurol Sci 1997;145:205–11.
[16] Matsuda H, Tsuji S, Shuke N, Sumiya H, Tonami N, Hisada K. Noninvasive measurements of regional cerebral blood flow using technetium-99 m hexamethylpropylene amine oxime. Eur J Nucl Med 1993;20:391–401.
[17] Matsuda H, Yagishita A, Tsuji S, Hisada K. A quantitative approach to technetium-99 m ethyl cysteinate dimer: a comparison with technetium-99 m hexamethylpropylene amine oxime. Eur J Nucl Med 1995;22:633–7.
[18] Lassen NA, Andersen AR, Friberg L, Paulson OB. The retention of [99mTc]-D,L-HMPAO in the human brain after intracarotid bolus injection: a kinetic analysis. J Cereb Blood Flow Metab 1988;8:S13–22.
[19] Friberg L, Andersen AR, Lassen NA, Holm S, Dam M. Retention of 99mTc-bicisate in the human brain after intracarotid injection. J Cereb Blood Flow Metab 1994;14:S19–27.
[20] Honjo K, Ohshita T, Kawakami H, Naka H, Imon Y, Maruyama H, et al. Quantitative assessment of cerebral blood flow in genetically confirmed spinocerebellar ataxia type 6. Arch Neurol 2004;61:933–7.
[21] De Michele G, Mainenti PP, Soricelli A, et al. Cerebral blood flow in spinocerebellar degenerations: a single photon emission tomography study in 28 patients. J Neurol 1998;245:603–8.
[22] LeWitt PA, Ehrenkranz JRL. TRH and spinocerebellar degeneration. Lancet 1982;2:981.
[23] Hökfelt T, Fuxe K, Johansson O, Jeffcoate S, White N. Distribution of thyrotropin-releasing hormone (TRH) in the central nervous system as revealed with immunohistochemistry. Eur J Pharmacol 1975;34(2):389–92.
[24] Kubek MJ, Lorincz MA, Wilber JF. The identification of thyrotropin releasing hormone (TRH) in hypothalamic and extrahypothalamic loci of the human nervous system. Brain Res 1977;126:196–200.
[25] Oturai PS, Friberg L, Sam I, Perrild H. Effects of thyrotropin-releasing hormone on regional cerebral blood flow in man. Acta Endocrinol (Copenh) 1992;126(3):243–6.
[26] Koskinen LO. Effect of low intravenous doses of TRH, acid-TRH and cyclo(His-Pro) on cerebral and peripheral blood flows. Br J Pharmaco 1986;87:509–19.
[27] Rouiller EM, Liang F, Babalian A, Moret V, Wiesendanger M. Cerebellothalamocortical and pallidothalamocortical projections to the primary and supplementary motor cortical areas: a multiple tracing study in macaque monkeys. J Comp Neurol 1994;345:185–213.
[28] Koskinen LO, Bill A. Thyrotropin-releasing hormone (TRH) causes sympathetic activation and cerebral vasodilation in the rabbit. Acta Physiol Scand 1984;122:127–36.
[29] Koskinen LO. Effects of TRH on cerebral and peripheral blood flows; role of submesencephalic brain stem centres. Acta Physiol Scand Oct 1986;128(2):277–88.
[30] Yarbrough GG. On the neuropharmacology of thyrotropin releasing hormone (TRH). Prog Neurobiol 1979;12:291–312.
[31] Inanami O, Meguro K, Ohno K, Sato A. Contribution of cholinergic vasodilators on the increase in cerebral cortical blood flow responses to the intravenous administration of thyrotropin releasing hormone in anesthetized rats. Neurosci Lett 1988;88:184–8.

Clinical Neurology and Neurosurgery 111 (2009) 296–299

Contents lists available at ScienceDirect

Clinical Neurology and Neurosurgery

journal homepage: www.elsevier.com/locate/clineuro

Case report

Monofocal large inflammatory demyelinating lesion, mimicking brain glioma

Noriyuki Kimura*, Toshihide Kumamoto, Takuya Hanaoka, Yusuke Hasama, Kenichiro Nakamura, Toshio Okazaki

Department of Neurology and Neuromuscular Disorders, Oita University, Faculty of Medicine, Idaigaoka 1-1, Hasama, Yufu, Oita 879-5593, Japan

ARTICLE INFO

Article history:
Received 5 May 2008
Received in revised form 5 October 2008
Accepted 7 October 2008

Keywords:
Monofocal demyelinating lesion
Glioma
Brain MRI
Steroid therapy
Brain biopsy

ABSTRACT

Here we report two cases of pathologically confirmed tumor-like demyelinating lesions. In comparison with common primary demyelinating diseases, our cases demonstrated atypical radiologic features, such as a large monofocal lesion with mild brain edema, and open ring-like or focal enhancement on magnetic resonance images, suggesting brain tumors. The clinical manifestations included focal neurologic signs due to the lesions, monophasic episodes without relapse over a long follow-up period, and efficacy of oral corticosteroid therapy. Histological analysis of brain biopsy specimens showed the inflammatory demyelination and preserved axons without tumor cells. The present cases suggest the importance of considering inflammatory demyelinating disease in the different diagnosis of monofocal tumor-like lesion.

1. Introduction

A tumor-like demyelinating lesion is a rare and unique radiologic finding. They appear as a large monofocal or multifocal contrast-enhancing lesions, and are often indistinguishable from brain tumors on computed tomography or magnetic resonance imaging (MRI) [1,2]. The clinical findings of such lesions are characterized by a rapidly progressive clinical course and neurologic symptoms, such as headaches, seizures, and unconsciousness [3,5–7]. These findings often lead to an incorrect or delayed diagnosis and treatment. Thus, it is crucial to confirm the correct diagnosis as inflammatory demyelinating disease.

In the present study, we report two cases of tumor-like demyelinating lesions. Each case presented a large monofocal lesion, which was initially diagnosed as glioblastoma or low-grade glioma, but the pathologic findings demonstrated the inflammatory demyelinating process. The clinical features revealed the gradually progress of neurologic symptoms and signs, the improvement of the clinical and radiologic abnormalities following treatment with high-dose oral prednisolone, and the development of neither new symptoms nor lesions during the long follow-up period. Similar cases were previously described and termed tumor-like demyelinating lesions or monofocal acute inflammatory demyelination (MAID) [3–11].

Here, we discuss the clinical manifestations and pathophysiology of these cases together with a review of the relevant literature.

2. Case report

2.1. Case 1

In January 2003, a 53-year-old, right-handed Japanese male developed a visual field deficit and left hemiparesis. He consulted a local physician for the progress of hemiparesis over the course of 1 month. Radiologic analysis revealed the presence of a mass lesion, which was initially suspected to be a malignant glioma, and stereotactic biopsy of the mass was performed. Because the histologic diagnosis was consistent with inflammatory demyelinating disease, the patient was referred to our hospital for further evaluation. He had a history of diabetes mellitus and diabetic neuropathy. In addition, he had no history of preceding viral infection or immunization prior to the onset of his current symptoms. On admission, neurologic examination revealed homonymous hemianopsia, vertical gaze palsy, left hemifacial palsy, and moderate left hemiparesis, with the lower extremity being more severely affected. His deep reflexes were decreased, presumably due to diabetic neuropathy, but the left Chaddock sign was positive. Hypesthesia was noted on the left side of the body and extremities. Routine blood tests were normal. Analysis of the cerebrospinal fluid (CSF) showed the increase of total protein (139 mg/dl; normal < 40 mg/dl), and myelin basic protein (MBP) (224 pg/ml; normal < 102 pg/ml). The immunoglobulin (Ig) G in CSF

* Corresponding author. Tel.: +81 97 586 5814; fax: +81 97 586 6502.
E-mail address: noriyuki@med.oita-u.ac.jp (N. Kimura).

0303-8467/$ – see front matter © 2008 Elsevier B.V. All rights reserved.
doi:10.1016/j.clineuro.2008.10.010

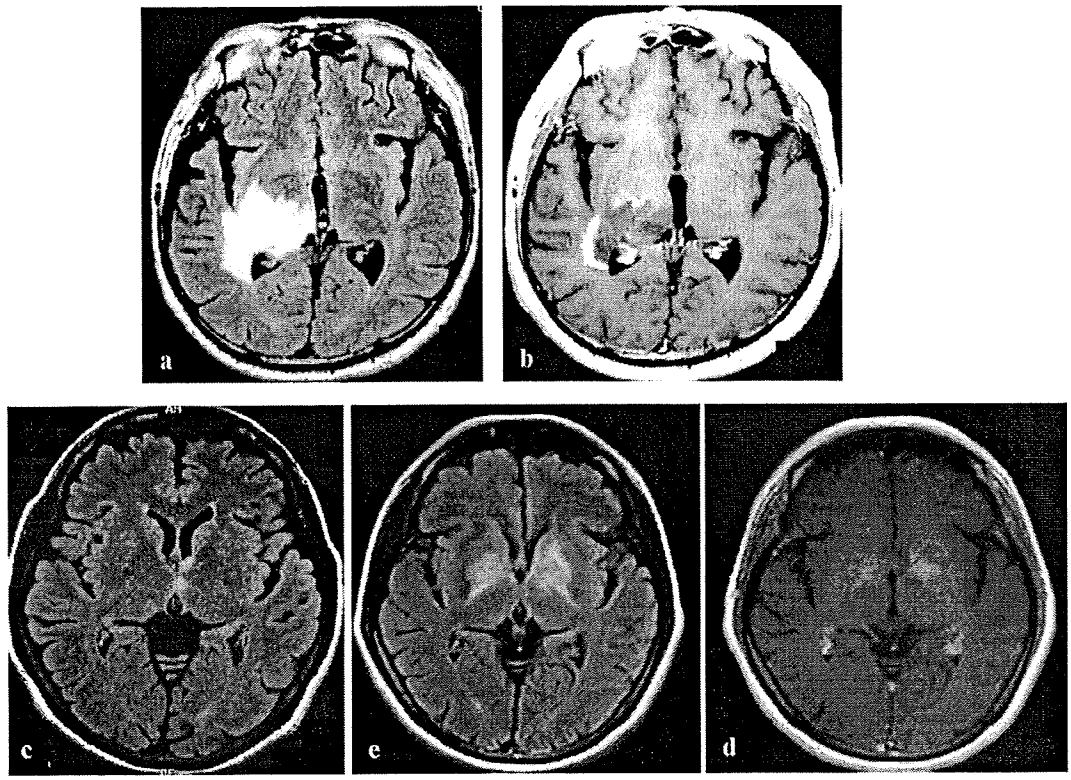

Fig. 1. Cranial MRI in case 1 (a and b) and case 2 (c–e). The right side is shown on the left-hand side of each figure. (a) Axial FLAIR image, obtained on admission, shows a large monofocal, hyperintense lesion with mild edema in the subependymal white matter of the right temporal lobe. (b) Axial gadolinium-enhanced T1-weighted image demonstrates open ring-like enhancement. (c) Axial FLAIR image, obtained at first examination, shows a small abnormal lesion in the left genu of the internal capsule and hypothalamus. (d) Follow-up axial FLAIR image, obtained on admission, shows a butterfly-shaped hyperintense lesion in the bilateral basal ganglia and the internal capsule without peripheral edema. (e) Axial gadolinium-enhanced T1-weighted image demonstrates focal contrast enhancement.

index was normal and oligoclonal bands were negative. Bacterial and fungal cultures were negative and no marked increase in antiviral titers in the serum or CSF was observed. Electroencephalogram (EEG) showed slow waves in the right temporal region. In March 2003, fluid-attenuated inversion recovery (FLAIR) MRI detected a large monofocal, hyperintense lesion. Gadolinium-enhanced MRI showed open ring-like enhancement in the subependymal white matter of right temporal lobe, which extended to the basal ganglia and midbrain (Fig. 1a and b). However, the peripheral edema and mass effect were disproportionately mild for the size of the lesion. MRI of the cervical, thoracic, or lumbar spine revealed no remarkable changes. The patient was treated with a high dose of oral prednisolone, 60 mg/day. Follow-up examination at 1 month revealed no abnormal neurologic symptoms. Two months later, repeated MRI revealed the absence of gadolinium enhancement and a decrease in the size of the periventricular lesion. He was discharged on a tapered dose of prednisolone and no relapse occurred during 5 years of follow-up.

2.2. Case 2

In December 2004, a 49-year-old, right-handed Japanese woman consulted a neurologist because of weakness in her right extremities over the preceding 2 weeks. Her medical and family history was unremarkable. Brain MRI showed a small abnormal lesion in the left genu of the internal capsule and the hypothalamus (Fig. 1c). Two months later, repeated MRI demonstrated that the lesion had extended to the ipsilateral lentiform nucleus and the contralateral basal ganglia through the anterior commissure. In mid-May, she was admitted to our hospital. On admission, the patient was drowsy and scored 10/30 on the Mini-Mental State examination (MMSE). She had mild weakness, rigidity, and hyperreflexia in the right extremities without pathologic reflex. Routine blood tests were normal. CSF analysis showed the increase of leukocyte count (39 mm^{-3}) and MBP level (124 pg/ml). EEG revealed diffuse slow waves. Repeated MRI demonstrated a butterfly-shaped lesion in the bilateral basal ganglia, characterized by a high-intensity signal on FLAIR images without edema and mass effect (Fig. 1d). Gadolinium-enhanced MRI showed focal contrast enhancement in the globus pallidus (Fig. 1e). She was initially treated with intravenous pulse methylprednisolone (1000 mg/day) for 3 days and high-dose oral prednisolone (60 mg/day). Although her CSF profiles returned to normal, cognitive impairment and right hemiparesis became worse over 1 month. Therefore, a butterfly glioma was suspected and a stereotactic brain biopsy was performed to verify the diagnosis. Histologic examination showed the inflammatory demyelinating lesion. High-dose oral prednisolone (60 mg/day) was continued and her neurologic symptoms gradually improved. Three months after initiation of the corticosteroid therapy, her neurologic symptoms returned to normal and MRI revealed the absence of gadolinium enhancement and a decrease in the size of the lesion. She was discharged on a tapered dose of prednisolone, and no relapse occurred during 2 years of follow-up.

2.3. Pathologic findings

The pathologic changes observed in case 1 (Fig. 2a–f) were more severe than those in case 2 (Fig. 2g and h), although both

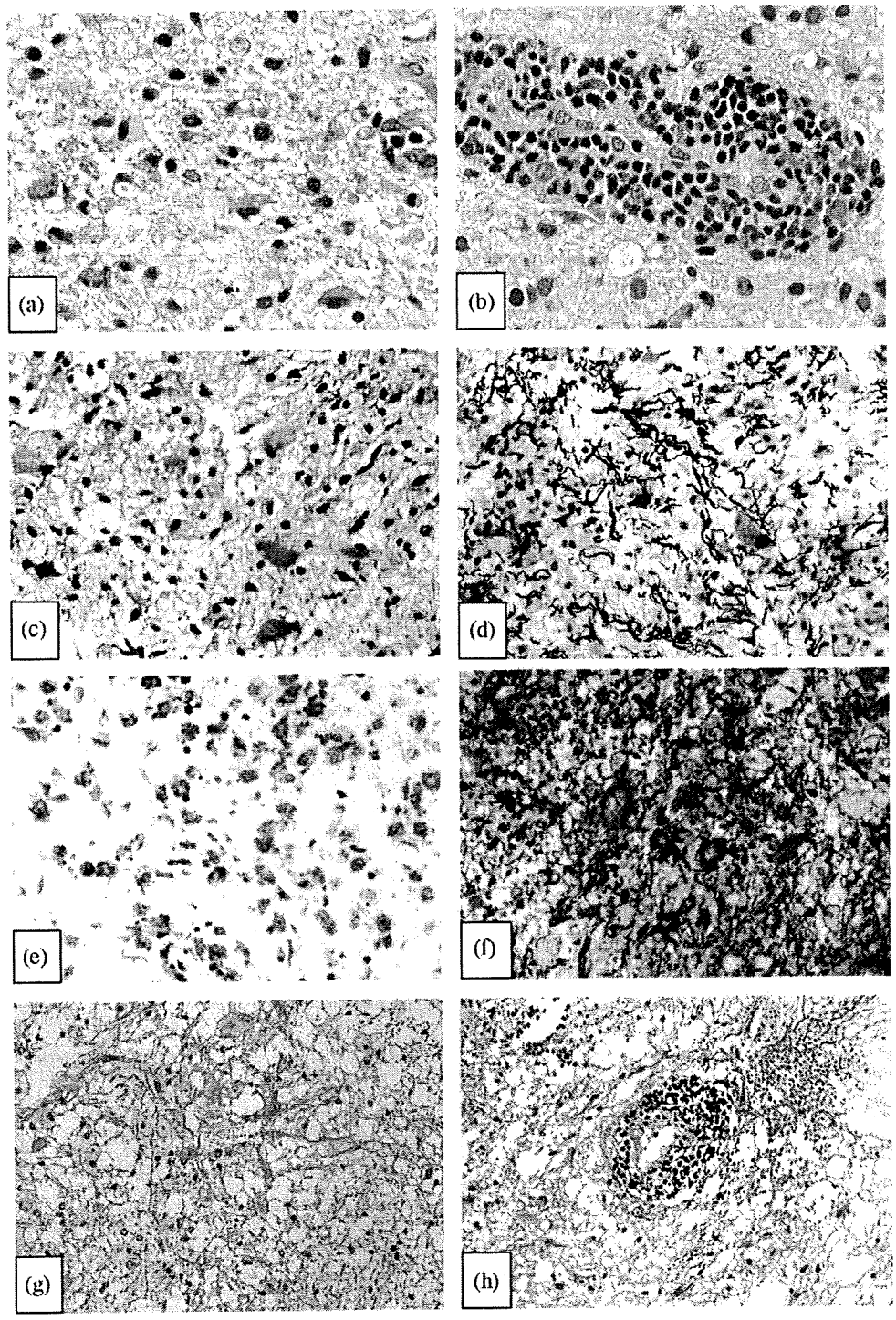

Fig. 2. Pathologic findings of the biopsy specimen obtained from case 1 (a–f) and case 2 (g–J). (a) Proliferation of numerous foamy macrophages and gemistocytic astrocytes (HE stain, 200×). (b) Massive perivascular lymphocyte cuffing (HE stain, 200×). (c) Severe myelin loss in areas infiltrated by macrophages, positive for myelin debris (Kluver–Barrera stain, 200×). (d) Relative preservation of axons in the lesion despite the myelin pallor (modified Bielschowsky stain, 200×). (e) Numerous foamy macrophages positive for CD 68 (200×). (f) Numerous gemistocytic astrocytes positive for GFAP (200×). (f) Proliferation of foamy macrophages and some reactive astrocytes (HE stain, 100×). (g) Moderate perivascular lymphocyte cuffing (HE stain, 100×).

cases shared marked morphologic similarities. The biopsy specimen was small and originated form the gadolinium-enhanced lesions. Hematoxylin and eosin (HE) staining revealed the severe tissue rarefaction with numerous foamy macrophages, and the intensive active gliosis with gemistocytic astrocytes proliferation throughout the lesions (Fig. 2a and g). Perivascular lymphocyte cuffing was observed at the periphery of the lesion, but there was no evidence of neovascularization (Fig. 2b and h). The characteristic

pathological findings of MS, such as the sharp border of the lesions and shadow plaques, could not be identified because of the near-total tissue rarefaction with diffuse infiltration of macrophages. Kluver–Barrera (KB) staining sowed severe myelin loss, and the broken-down myelin fragments in the cytoplasm of macrophage were observed (Fig. 2c). In contrast to the myelin pallor, modified Bielschowsky staining showed relatively well-preserved axons in the lesions (Fig. 2d). Numerous foamy macrophages were positive staining for CD68 (PMG1 monoclonal, diluted 1:200; Dako, Glostrup, Denmark) (Fig. 2e), and the gemistocytic astrocytes were positive staining for glial fibrillary acidic protein (GFAP, polyclonal; Dako, Denmark) within and around the lesion (Fig. 2f). Neither atypical cells nor any findings suggestive of a tumor was detected. These pathologic findings confirmed the diagnosis of active inflammatory demyelinating disease.

3. Discussion

We describe two cases with atypical clinical and MRI features of demyelinating lesions that resembled a glioblastoma and a butterfly shaped low-grade glioma. The present cases demonstrated the increase of protein level, MBP, or leukocyte count in CSF analysis and a large monofocal lesion with disproportionately mild or no peripheral edema or open ring-like enhancement on MRI, suggesting an ongoing inflammatory demyelinating process [2,12]. Stereotactic biopsy however was necessary to confirm the correct diagnosis because of the progressive clinical signs, initial unresponsiveness to corticosteroid treatment, and an actively growing lesion. The common pathologic findings of our cases were characterized by the severe myelin loss with relatively well-preserved axons, numerous foamy macrophages, proliferation of reactive astrocytes, and perivascular lymphocyte cuffing that are consistent with the inflammatory demyelinating plaque. Therefore, we speculate that the same immunologic mechanism participate in the development of these lesions, although the clinical and radiological findings were different.

In the previous reports, several demyelinating diseases, such as MS [13,14], acute disseminated encephalomyelitis (ADEM) [15], and myelinoclastic diffuse sclerosis (MDS) [16,17] sometimes presented with tumor-like lesions. MS is the most common form of primary demyelinating disease and the diagnosis largely depends on the clinical course, which is characterized by relapsing–remitting or progressive neurologic deficits. Unlike MS, ADEM is a monophasic inflammatory demyelinating disease, usually preceded by systemic viral infection or vaccination. Solitary or multiple lesions are distributed throughout the cerebral white matter, and frequently involve cortical and deep gray matter. MDS is a monophasic demyelinating disease that occurs mainly in children and demonstrates one or two symmetric bilateral lesions involving the centrum semiovale [16]. Our cases presented with no history of virus infection or vaccination, and monophasic clinical or radiologic deficits over long follow-up period. The monofocal lesion located in the right temporal white matter and bilateral basal ganglia without preference for periventricular area. Therefore, they did not clearly fit the diagnostic criteria for MS, ADEM, or MDS with regard to the clinical course and the location of lesions. In literature, similar cases were described and termed tumor-like demyelinating lesions or monofocal acute inflammatory demyelination (MAID) [3–11]. Clinical features of these cases show the acute onset of focal neurologic signs and normal CSF analysis except for the increase of protein or MBP levels in a few cases. Most of the cases demonstrated a good response to steroid therapy and monophasic episodes without relapse during long follow-up periods. The precise nosologic classification of these patients remains uncertain. Gutrecht et al. [7] suggested that MAID may be a unique form of acute, monofocal, cerebral demyelinating disease that appears to be more similar to ADEM than to MS. Moreover, some patients with MAID may have immunologic characteristics that prevent MS from developing. Poser et al. [2,16] considered tumor-like demyelinating lesions as variants of MS, whereas Kepes [1] suggested that they occupy an intermediate position between MS and ADEM. In our cases, the clinical course and radiologic findings favored ADEM except for no history of systemic viral infection or vaccination, lesion sizes however exceed that of the small foci of perivenous demyelination seen in typical ADEM. Moreover, pathologic features were consistent with those of the previous cases of tumor-like MS [13,14]. Therefore, present cases were similar to the published cases with tumor-like demyelinating lesions, which may represent an entity intermediate between MS and ADEM. We speculate that the same immunologic mechanisms may contribute to the pathogenesis of monofocal tumor-like demyelinating lesion.

In conclusion, we suggest that the inflammatory demyelinating disease should be considered, even if the patients with monofocal tumor-like lesions demonstrate the slowly progressive clinical course. Long term oral prednisolone therapy may be effective in these patients. Brain biopsy is a considered a diagnostic procedure for the correct diagnosis of tumor-like lesions and can contribute to the appropriate treatment.

References

[1] Kepes JJ. Large focal tumor-like demyelinating lesions of the brain: intermediate entity between multiple sclerosis and acute disseminated encephalomyelitis? A study of 31 patients. Ann Neurol 1993;33(1):18–27.
[2] Dagher AP, Smirniotopoulos J. Tumefactive demyelinating lesions. Neuroradiology 1996;38(6):560–5.
[3] Kalyan-Raman UP, Garwacki DJ, Elwood PW. Demyelinating disease of corpus callosum presenting as glioma on magnetic resonance scan: a case documented with pathological findings. Neurosurgery 1987;21(2):247–50.
[4] Censori B, Agostinis C, Partziguian T, Gazzaniga G, Biroli F, Mamoli A. Large demyelinating brain lesion mimicking a herniating tumor. Neurol Sci 2001;22(4):325–9.
[5] Heyman D, Delhaye M, Fournier D, Mercier P, Rousselet MC, Menei P. Pseudotumoral demyelination: a diagnosis pitfall (report of three cases). J Neurooncol 2001;54(1):71–6.
[6] Sugita Y, Terasaki M, Shigemori M, Sakata K, Morimatsu M. Acute focal demyelinating disease simulating brain tumors: histopathologic guidelines for an accurate diagnosis. Neuropathology 2001;21(1):25–31.
[7] Gutrecht JA, Berger JR, Jones Jr RH, Mancall AC. Monofocal acute inflammatory Demyelination (MAID): a unique disorder simulating brain neoplasm. South Med J 2002;95(1):1180–6.
[8] Tan HM, Chan LL, Chuah KL, Goh NS, Tang KK. Monophasic, solitary tumefactive demyelinating lesion: neuroimaging features and neuropathological diagnosis. Br J Radiol 2004;77(914):153–6.
[9] Mandrioli J, Ficarra G, Callari G, Sola P, Merelli E. Monofocal acute large demyelinating lesion mimicking brain glioma. Neurol Sci 2004;25:S386–8.
[10] Enzinger C, Strasser-Fuchs S, Ropele S, Kapeller P, Kleinert R, Fazekas F. Tumefactive demyelinating lesions: conventional and advanced magnetic resonance imaging. Mult Scler 2005;11(2):135–9.
[11] Akimoto J, Nakajima N, Saida A, Haraoka J, Kudo M. Monofocal acute inflammatory demyelination manifesting as open ring sign. Case report. Neurol Med Chir (Tokyo) 2006;46(7):353–7.
[12] Masdeu JC, Quinto C, Olivera C, Tenner M, Leslie D, Visintainer P. Open-ring imaging sign: highly specific for atypical brain demyelination. Neurology 2000;54(7):1427–33.
[13] Nesbit GM, Forbes GS, Scheithauer BW, Okazaki H, Rodriguez M. Multiple sclerosis: histopathologic and MR and/or CT correlation in 37 cases at biopsy and three cases at autopsy. Radiology 1991;180(2):467–74.
[14] Di Patre PL, Castillo V, Delavelle J, Vuillemoz S, Picard F, Landis T. "Tumor-mimicking" multiple sclerosis. Clin Neuropathol 2003;22(5):235–9.
[15] Singh S, Alexander M, Sase N, Korah IP. Solitary hemispheric demyelination in acute disseminated encephalomyelitis: clinicoradiological correlation. Australas Radiol 2003;47(1):29–36.
[16] Poser CM, Goutières F, Carpentier MA, Aicardi J. Schilder's myelinoclastic diffuse sclerosis. Pediatrics 1986;77(1):107–12.
[17] Afifi AK, Bell WE, Menezes AH, Moore SA. Myelinoclastic diffuse sclerosis (Schilder's disease): report of a case and review of the literature. J Child Neurol 1994;9(4):398–403.

INTERNAL MEDICINE

□ CASE REPORT □

Acute Encephalomyelitis Associated with Acute Viral Hepatitis Type B

Keiko Kinomoto[1], Yoshinobu Okamoto[2], Yuichiro Yuchi[2] and Masaru Kuriyama[1]

Abstract

We describe the case of a 36-year-old woman who developed acute encephalo-myelitis after acute viral hepatitis type B. She was admitted to the hospital with a history of general malaise and nausea of 5 days duration. Her serum showed high transaminase levels and positive HBs-Ag and increased IgM HBc-Ab titers. She had urinary dysfunction, myoclonus and postural tremor of her extremities. Several days later, she developed bilateral limb ataxia and alteration of consciousness. The cerebrospinal fluid examinations showed pleocytosis and increased protein. Treatment with high-dose methylprednisolone resulted in a marked improvement of the clinical and CSF examination. Magnetic resonance imaging of the brain and the spinal cord did not disclose abnormal lesions. The symptoms and clinical course were quite similar to those of acute disseminated encephalomyelitis.

Key words: acute disseminated encephalomyelitis (ADEM), acute viral hepatitis, hepatitis B virus (HBV)

(Inter Med 48: 241-243, 2009)
(DOI: 10.2169/internalmedicine.48.1641)

Introduction

Acute disseminated encephalomyelitis (ADEM) is an autoimmune demyelinating disease of the central nervous system that generally develops after acute viral or bacterial infection or vaccination (1-3). ADEM is usually a monophasic disease with acute onset characterized by multiple foci of central nervous system damage, predominantly in the cerebral and cerebellar white matter, although basal ganglia and gray matter may also be involved. Lesions are frequently bilateral, large, and confluent (1-3). Numerous infectious agents have been linked to ADEM. A search of the literature revealed some reports of cases associated with hepatitis A virus infection and hepatitis C virus infection (4, 5). Regarding hepatitis B virus, however, no association of hepatitis B virus infection with acute disseminated encephalomyelitis have been reported despite the fact that some cases associated with hepatitis B virus vaccination have been reported (6-8). Furthermore, the possibility that hepatitis B vaccine may cause or exacerbate multiple sclerosis (MS) stems from several reports of onset or recurrence of symptoms of CNS demyelination shortly after vaccination (9). We describe the case of a 36-year-old woman who developed acute encephalomyelitis after acute viral hepatitis type B, and discuss the pathogenesis of the disturbance.

Case Report

A 36-year-old woman was admitted to the Department of Internal Medicine, Maizuru Kyousai Hospital with a history of general malaise and nausea of 5 days duration. There was no history of toxic substance or drug ingestion. On admission, the serum transaminase (AST; 355 IU/L, ALT; 1,916 IU/L) and γ-GTP (357 IU/L) levels were elevated. WBC level (10,600/μL) in blood was slightly increased. Other routine laboratory examinations including anti-nuclear antibody (ANA), anti-DNA antibody, P-ANCA and C-ANCA were all normal or negative. Hepatitis Bs antigen (48.08) and IgM hepatitis B core antibody (IgM HBc-Ab) were positive. IgMHA-Ab,HCV-Ab, EBV VCAIgG (320), EBVVCAIgM (<10), EBNA (160) were all not significantly increased or negative. She was diagnosed as acute hepatitis B. She showed no signs of neurological deficient. Findings of elec-

[1]The Second Department of Internal Medicine (Neurology Division), Faculty of Medical Science, University of Fukui, Fukui and [2]Department of Internal Medicine, Maizuru Kyosai Hospital, Maizuru
Received for publication August 28, 2008; Accepted for publication September 30, 2008
Correspondence to Dr. Masaru Kuriyama, masa@u-fukui.ac.jp

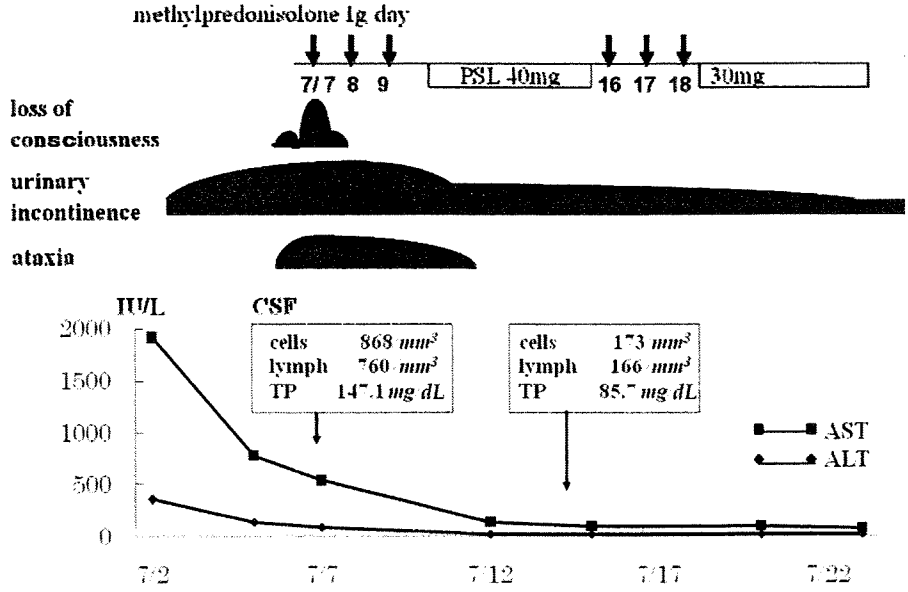

Figure 1. Clinical course of the patient.

trocardiograph and chest x-ray film examinations were normal. Ten hours later, she developed urinary dysfunction. On the second day of the admission she showed myoclonus on the inside of her thighs and postural tremor of her upper extremities. On the 10th day of admission, she developed bilateral limb ataxia and on the following day she developed alteration of consciousness. The cerebrospinal fluid examinations showed pleocytosis (868/mm^3) composed of 760/mm^3 mononuclear cells and 108/mm^3 polynuclear cells and increased total protein (147 mg/dL). Glucose in CSF was 51 mg/dL. Bacterial, mycobacterial, and fungal cultures from cerebrospinal fluid were negative. Magnetic resonance imaging (MRI) of the brain and the spinal cord revealed no abnormal findings. Gadolinium contrast enhancement MRI was not examined in this patient.

Treatment with high-dose methylprednisolone was followed by a dramatic improvement of the clinical and cerebrospinal fluid findings. The clinical course is shown in Fig. 1. Within a few months the patient recovered completely and there was no relapse during 1 year of follow-up.

Discussion

ADEM is a monophasic disease that occurs in the setting of infection or immunization. The pathological characteristics of the condition are perivascular inflammation, edema and demyelination in the central nervous system. After prodromal phase of 1-4 weeks, clinical signs including altered consciousness and multifocal neurological disturbance appear. Moderate pleocytosis in the cerebrospinal fluid is a common feature but, in contrast with multiple sclerosis, oligoclonal bands are rarely obserbed (10). MRI is considered the diagnostic tool of choice for suspected ADEM (1, 2, 3, 11). In our case, the clinical signs and symptoms combined with the serum and cerebrospinal fluid findings and the clinical marked improvement with corticosteroid therapy were strongly suggestive of ADEM, though MRI could not disclose abnormal findings in the brain or the spinal cord. The incidence of lesions on MRI is variable in ADEM and may depend on the stage of inflammation. Gadolinium enhancing lesions have been described in 30 to 100% of patients. As spinal cord involvement in ADEM has been described in 11 to 28%, spinal cord lesions could be rarely disclosed on MRI (3).

In the present case, apart from the indication of a recent hepatitis virus B infection, laboratory investigation revealed no infection or infectious agent. In recent years, several reports of new cases of central nervous system demyelination or reactivation of multiple sclerosis after hepatitis B vaccination have raised the possibility of a causal link (6-8). In addition, it was reported that hepatitis virus B polymerase shares significant amino acid similarities with the human myelin basic protein (12). However, our search of the literature revealed no previously reported case of ADEM following this infection.

There could be two possibilities, demyelination or vasculitis, for the pathogenetic mechanism of neurological involvement in this case. In general, vasculitis associated with hepatitis viral infection has occurred in the chronic stage, especially in chronic hepatitis type C (13, 14). In some patients with chronic hepatitis type C and B, complicated secondary cryoglobulinemia or polyartilitis nodosa induced damage of the blood vessels, resulting in vasculitic neuropathy (15). The CNS disorders as a complication of hepatitis rarely occur in patients with hepatitis type B, who were also in the chronic stage (15-17). In the present patient, acute onset CNS neurological deficits with CSF pleocytosis occurred shortly after the infection of hepatitis B virus, and steroid therapy showed marked effect for the disturbances. These findings suggest that the pathogenesis in this case could be

due to a demyelinating process, rather than vasculitis.

This case shows that ADEM-like CNS neurological involvement can be associated with hepatitis virus B infection. We emphasize the importance of hepatitis virus B screening in patients with acute encephalomyelitis, since many cases of hepatitis virus B infection remain anicteric or subclinical. Likewise, patients with hepatitis virus B infection should be examined carefully for central nervous system symptoms during follow-up.

References

1. Rust RS. Multiple sclerosis, acute disseminated encephalomyelitis and related conditions. Semin Pediatr Neurol **7**: 66-90, 2000.
2. Tenenbaum S, Chamoles N, Fejerman N. Acute disseminated encephalomyelitis: a long-term follow-up study of 84 pediatric patients. Neurology **59**: 1224-1231, 2002.
3. Tenembaum S, Chitnis T, Ness J, Hahn JS. Acute disseminated encephalomyelitis. Neurology **68** (Suppl 2): S23-S36, 2007.
4. Alehan FK, Kahveci S, Uslu Y, Yildirim T, Yilmaz B. Acute disseminated encephalomyelitis associated with hepatitis A virus infection. Ann Trop Paediatr **24**: 141-144, 2004.
5. Sacconi S, Salviati L, Merelli E. Acute disseminated encephalomyelitis associated with hepatitis C virus infection. Arch Neurol **58**: 1679-1681, 2001.
6. Schattner A. Consequence or coincidence? The occurrence, pathogenesis and significance of autoimmune manifestations after vaccines. Vaccine **23**: 3876-3886, 2005.
7. Herroelen L, de Keyser J, Ebinger G. Central nervous system demyelination after immunization with recombinant hepatitis B vaccine. Lancet **338**: 1174-1175, 1991.
8. Gout O, Theodorou I, Liblau R, Lyon-Caen O. Central nervous system demyelination after recombinant hepatitis B vaccination. Report of 25 cases. Neurology **48**: A424, 1997 (abstract.).
9. DeStefano F, Verstraeten T, Chen RT. Hepatitis B and risk of multiple sclerosis. Expert Rev Vaccines **1**: 461-466, 2002.
10. Hynson JL, Kornberg AJ, Coleman LT, Shield L, Harvey AS, Kean MJ. Clinical and neuroradiological features of acute disseminated encephalomyelitis in children. Neurology **56**: 1308-1312, 2001.
11. Kesselring J, Miller DH, Robb SA, et al. Acute disseminated encephalomyelitis: MRI findings and the distinction from multiple sclerosis. Brain **113**: 291-302, 1990.
12. Faure E. Multiple sclerosis and hepatitis B vaccination: Could minute contamination of the vaccine by partial Hepatitis B virus polymerase play a role through molecular mimicry? Medical Hypothesis **65**: 509-520, 2005.
13. Casato M, Saadoun D, Marchetti A, et al. Central nervous system involvement in hepatitis C virus cryoglobulinemia vasculitis: a multicenter case-control study using magnetic resonance imaging and neuropsychological tests. J Rheumatol **32**: 484-488, 2005.
14. Cacoub P, Saadoun D, Limal N, Léger JM, Maisonobe T. Hepatitis C virus infection and mixed cryoglobulinaemia vasculitis: a review of neurological complications. AIDS **19** Suppl 3: S128-S134, 2005.
15. Cohen P, Guillevin L. Vasculitis associated with viral infections. Presse Med **33**: 1371-1384, 2004.
16. Matsui M, Kakigi R, Watanabe S, Kuroda Y. Recurrent demyelinating transverse myelitis in a high titer HBs-antigen carrier. J Neurol Sci **139**: 235-237, 1996.
17. Aprosina ZG, Borisova VV, Krel' PE, Serov VV, Sklianskaia OA. The unique course of a chronic generalized infection with the hepatitis B virus (a clinico-morphological observation). Ter Arkh **68**: 16-19, 1996.

Journal of the Neurological Sciences 285 (2009) 265–267

Contents lists available at ScienceDirect

Journal of the Neurological Sciences

journal homepage: www.elsevier.com/locate/jns

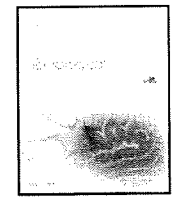

Short communication

Unique clinicopathological features and PrP profiles in the first autopsied case of dura mater graft-associated Creutzfeldt–Jakob disease with codon 219 lysine allele observed in Japanese population

Masamichi Ikawa [a], Makoto Yoneda [a,*], Akiko Matsunaga [a], Hiroto Nakagawa [a], Asuka Kazama-Suzuki [b], Nobuo Miyashita [b], Hironobu Naiki [c], Tetsuyuki Kitamoto [d], Masaru Kuriyama [a]

[a] Second Department of Internal Medicine (Neurology), Faculty of Medical Sciences, University of Fukui, 23-3 Shimoaiduki, Matsuoka, Eiheiji-cho, Yoshida-gun, Fukui 910-1193, Japan
[b] Department of Neurology, Koshigaya Municipal Hospital, 10-47-1 Higashi-Koshigaya, Koshigaya, Saitama 343-8577, Japan
[c] Department of Molecular Pathology, Faculty of Medical Sciences, University of Fukui, 23-3 Shimoaiduki, Matsuoka, Eiheiji-cho, Yoshida-gun, Fukui 910-1193, Japan
[d] Division of CJD Science and Technology, Department of Prion Research, Center for Translational and Advanced Animal Research on Human Diseases, Tohoku University Graduate School of Medicine, 2-1 Seiryo-cho, Aoba-ku, Sendai, Miyagi 980-8575, Japan

ARTICLE INFO

Article history:
Received 2 April 2009
Received in revised form 22 June 2009
Accepted 23 July 2009
Available online 8 August 2009

Keywords:
Dura mater graft-associated Creutzfeldt–Jakob disease
Codon 219 polymorphism
Glycosylation pattern in prion protein

ABSTRACT

Polymorphism at codon 219 lysine in prion protein (PrP) is considered to affect the clinicopathological features of prion diseases including Creutzfeldt–Jakob disease (CJD) and to have an inhibiting effect on the pathogenesis of these diseases. We describe the first autopsied case of dura mater graft-associated CJD (dCJD) with heterozygosity of lysine at codon 219 in PrP observed in a Japanese subject. Although this case demonstrated the non-plaque type of dCJD and MM1 subgroup of CJD pathologically and biochemically, the patient demonstrated a long incubation period (19.3 years), atypical periodic sharp-wave complexes with a dominant rhythm on EEG, partially scattered small deposits of plaque-like PrP along with synaptic type deposits of PrP on immunohistochemistry and an atypical MM1 glycosylation pattern with a relatively increased diglycosylated isoform of proteinase-resistant PrP on western blot analysis (*i.e.* "MM1 variant" pattern). These findings in this case were atypical of the non-plaque type of dCJD and MM1 subgroup of CJD. Thus, these findings can be unique to dCJD with codon 219 lysine allele, and this allele may influence the clinicopathological features and PrP profiles in dCJD.

1. Introduction

Human prion diseases including Creutzfeldt–Jakob disease (CJD) are caused by the abnormal accumulation of prion protein (PrP). PrP has a common polymorphism at codon 129, which is associated with the clinicopathological findings of these diseases [1]. Glutamate to lysine substitution at codon 219 in PrP is also a common polymorphism observed in the Asian population, especially in Japan, but has not been previously documented in sporadic CJD (sCJD) [2,3]. Additionally, codon 219 lysine allele with prion diseases has been detected only in genetic CJD (*i.e.* accompanied by pathogenic mutations in PrP) or iatrogenic CJD including dura mater graft-associated CJD (dCJD), and genetic CJD with this allele demonstrated atypical clinicopathological findings [4–7]. Thus, the codon 219 lysine allele is considered to not only inhibit the pathogenesis of prion diseases but also influence the clinicopathological features of these CJDs [3–9]. However, the pathological and biochemical features of dCJD with codon 219 lysine allele have not been reported to date. Here we report the first autopsied case of dCJD with codon 219 lysine allele observed in a Japanese subject, which presented unique clinicopathological features and PrP profiles.

2. Case report

A 35-year-old Japanese man developed insomnia and anxiety in September 2004, and subsequently developed gait disturbance, dysarthria and ataxia over the subsequent three months. He had undergone left frontal craniotomy to evacuate traumatic hematoma, and received a cadaveric dura mater graft (LYODURA^{R}, B. Braun, Germany) transplant in June 1985. There was no known family history of prion diseases. The patient was confused, and presented with nystagmus, dysarthria, dysphagia, rigidity, intention tremor and hyperreflexia in the extremities, and urinary incontinence at hospitalization in February 2005. Thereafter, 14-3-3 protein was detected in the CSF. Diffusion-weighted and fluid attenuation inversion recovery images on brain MRI demonstrated hyperintensities in the bilateral putamen, caudate and fronttemporal cerebral cortex, which were compatible with findings of CJD (Fig. 1A, B). EEG performed eight months after the onset showed atypical periodic sharp-wave complexes (PSWCs) with a dominant

* Corresponding author. Tel.: +81 776 61 8351; fax: +81 776 61 8110.
E-mail address: myoneda@u-fukui.ac.jp (M. Yoneda).

0022-510X/$ – see front matter © 2009 Elsevier B.V. All rights reserved.
doi:10.1016/j.jns.2009.07.019

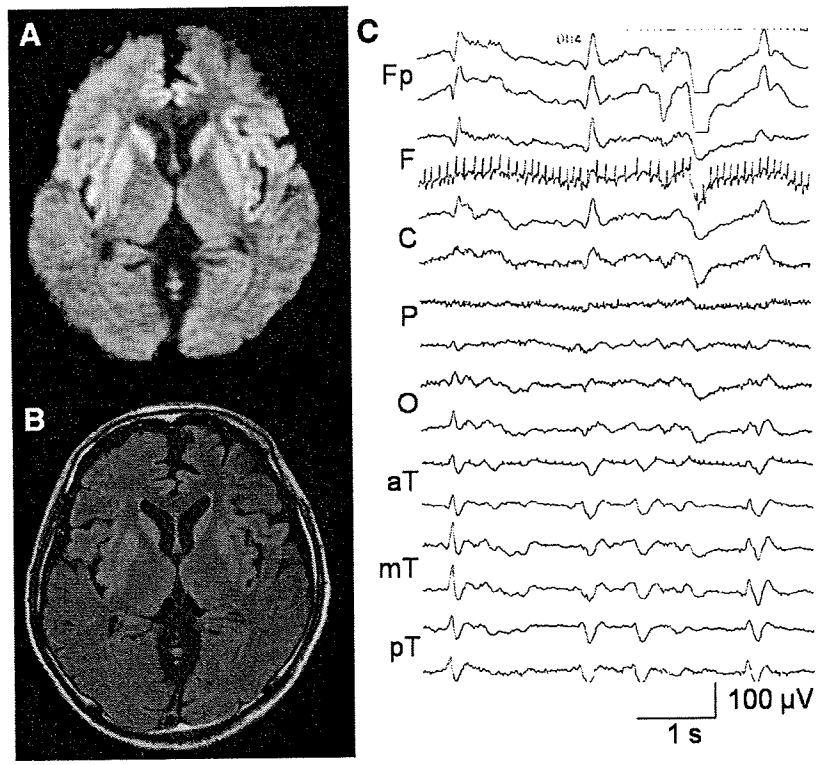

Fig. 1. Brain MRI and EEG findings. Hyperintensities were detected in the bilateral putamen, caudate and front-temporal cerebral cortex with slight atrophy on MR diffusion-weighted (A) and fluid attenuation inversion recovery (B) images obtained five months after onset. (C) EEG performed 8 months after onset showed atypical periodic sharp-wave complexes (PSWCs), but a dominant rhythm persisted. Fp = frontal pole; F = frontal; C = central; P = parietal; O = occipital; aT = anterior temporal; mT = mid-temporal; pT = posterior temporal.

rhythm (Fig. 1C). The open reading frame of PrP gene from the blood sample did not show any pathological mutation, a homozygote of methionine at codon 129 and a heterozygote of glutamate/lysine at codon 219. Written permission for PrP gene analysis was obtained from the patient's family. Six months after onset, he developed myoclonus in the extremities, and fell into akinetic mutism. Despite repeated EEG studies, typical PSWCs were not detected. He died of pneumonia in February 2006.

An autopsy was performed within 3 h after death. Written permission for autopsy was obtained from the patient's family. At autopsy, the brain weighed 995 g and showed marked atrophic change especially in the frontal lobes. Histological examination demonstrated significant neuronal loss and gliosis without typical spongiform changes in the cerebral cortex (Fig. 2A). Immunohistochemistry using anti-PrP monoclonal antibody 3F4 (Sigma-Aldrich, US) demonstrated that PrP deposits of the synaptic type in the cerebral and cerebellar cortex accompanied by partially scattered small deposits of plaque-like PrP, which were not typical amyloid plaque, in the white matter of the temporal lobes and hippocampi (Fig. 2B). Thus, this case was categorized into non-plaque type dCJD pathologically [10].

A western blot analysis of the protease K-treated autopsied brain homogenate probed with anti-PrP monoclonal antibody 3F4 demonstrated that the molecular weight of the unglycosylated isoform of proteinase-resistant PrP (PrP^{Sc}) was 21 kDa, which indicates type 1 PrP^{Sc} (*i.e.* MM1 subgroup of CJD) and non-plaque type dCJD [1,11]. The amount ratios of each isoform of PrP^{Sc} on western blot were quantified as the signal intensities of each corresponding band using Quantity One software in an imaging device, Vasa Doc 5000 (BioRad Laboratories, USA). The ratios of the diglycosylated isoform were increased in all samples obtained from the frontal cortex, cingulate gyrus and cerebellar cortex, compared with that in the typical MM1 subgroup of sCJD (Fig. 2C).

3. Discussion

We report the clinicopathological and biochemical features of the first autopsied case of dCJD with codon 219 lysine allele in PrP. This case was very briefly referenced in a surveillance report [10]. Although another case of dCJD was reported in a surveillance report as having the codon 219 lysine allele [7], this reported case did not undergo either histological or biochemical examinations, and only a few clinical findings were described in the previous report.

Codon 219 lysine allele has not been previously documented in sCJD [3]. Codon 218 lysine allele in mouse PrP (corresponding to codon 219 lysine allele in human PrP) inhibits the conversion to PrP^{Sc} in cultured cells, and heterozygous (*i.e.* glutamate/lysine) alleles at codon 219 in human PrP also had a protective effect on the conversion to PrP^{Sc} in knock-in mice [8,9]. Moreover, clinicopathological features in genetic CJD patients carrying codon 219 lysine allele were atypical of the classic form of each genetic CJD [4–6]. Therefore, codon 219 lysine allele is considered to have a resistant effect on the development of CJD, which influences clinicopathological and biochemical findings in CJD.

The present case belonged to the non-plaque type of dCJD and MM1 subgroup of CJD according to pathological and biochemical findings [1,10,11]. However, this case showed unique clinicopathological and biochemical findings as the non-plaque type in the MM1 subgroup (Table 1, Fig. 2C). This case had a long incubation period (19.3 years) compared with the average for the non-plaque type of dCJD (14.6 years) [10]. Although the surveillance report indicated that PSWCs had been detected with high frequency on EEG in the non-plaque type [10], repetitive EEGs in this case demonstrated atypical PSWCs with a persistent dominant rhythm, which differed from the typical PSWC findings in CJD (Fig. 1C). Immunohistochemistry in this case demonstrated partially scattered small deposits of plaque-like PrP, which has not previously been reported in the non-plaque type,

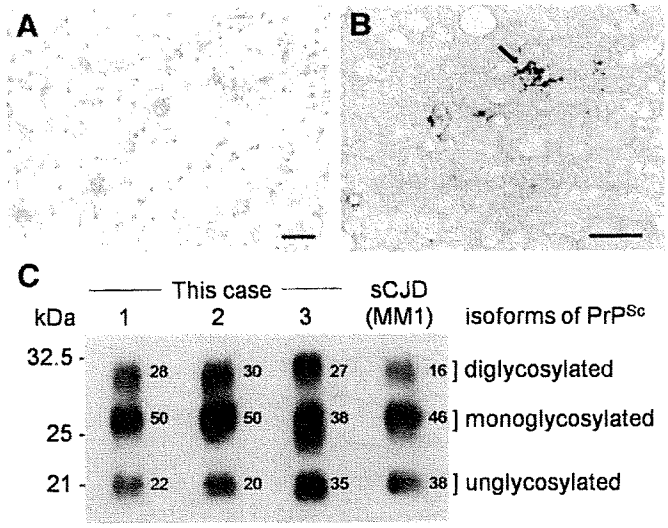

Fig. 2. Neuropathological findings and western blot analysis. (A) Histological analysis in the frontal cerebral cortex displayed marked neuronal loss and gliosis, without typical spongiform change (hematoxylin–eosin stain). (B) Immunohistochemical staining of prion protein (PrP) in the white matter of the temporal lobe showed scattered small deposits of plaque-like PrP (arrow) among the synaptic accumulation of PrP, without typical amyloid plaque. Scale bar = 50 μm. (C) Western blot analysis of protease K-resistant prion protein (PrP^{Sc}) fractions probed with anti-PrP monoclonal antibody 3F4 from the frontal cerebral cortex (lane 1), cingulate gyrus (lane 2) and cerebellar cortex (lane 3) in this case, and the frontal cerebral cortex in a case diagnosed as having the MM1 subgroup of sporadic CJD (lane of sCJD (MM1)). The western blot analysis demonstrated three major bands; the upper bands corresponded to diglycosylated isoform of PrP^{Sc}, the middle bands corresponded to monoglycosylated isoform and the lower bands corresponded to unglycosylated isoform. The numbers indicated by the side of each band corresponded to the ratios (%). The sCJD (MM1) lane showed a greater abundance of the monoglycosylated and unglycosylated isoforms compared to that of the diglycosylated isoform. Although this (the present) case and the sCJD (MM1) case both carried a homozygote of methionine at codon 129 in PrP and showed a type-1 pattern (21 kDa unglycosylated isoforms), the ratios of diglycosylated isoforms in this case were increased compared with those in the sCJD (MM1) case (*i.e.* "MM1 variant" pattern). PrP^{Sc} = proteinase-resistant PrP; MM1 = codon 129 methionine/methionine with type 1 PrP^{Sc}.

but similar plaque-like deposits were reported in genetic CJD with codon 219 lysine allele [4] (Fig. 2B). Although the MM1 subgroup demonstrated a large amount of monoglycosylated and unglycosylated isoforms of PrP^{Sc} compared with the diglycosylated isoform on western blot analysis in general [1], the ratios of diglycosylated isoform were increased in different areas of the autopsied brain in this case on quantitative analysis of each corresponding band (*i.e.* "MM1 variant" pattern) (Fig. 2C). This glycosylation pattern usually appears in MM2-C and VV2 subgroups, but does not usually appear in MM1 subgroup [1].

Therefore, a long incubation period, atypical PSWCs on EEG, small deposits of plaque-like PrP on immunohistochemistry in the non-plaque type and "MM1 variant" pattern on western blot analysis may be unique to dCJD with codon 219 lysine allele. Furthermore, the codon 219 lysine allele appears to influence the clinicopathological features and PrP profiles in dCJD.

Table 1
Clinicopathological manifestations in this case and non-plaque type of dCJD.

	This case		Non-plaque type of dCJD	
	Occurrence	Duration	Occurrence (%)	Duration (mean)
Incubation period		19.3 yrs.		14.6 yrs.
Age at onset		33 y/o		56.7 y/o
Clinical manifestations				
Cerebellar signs	+	3 mo.	75	0.6 mo.
Psychiatric symptoms	+	0 mo.	67	0.5 mo.
Dementia	+	5 mo.	100	0.9 mo.
Visual disturbance	−		42	0.4 mo.
Myoclonus	+	6 mo.	100	2.0 mo.
Extrapyramidal signs	+	5 mo.	42	2.2 mo.
Pyramidal signs	+	5 mo.	100	2.2 mo.
Akinetic mutism	+	6 mo.	92	2.8 mo.
Death	+	17 mo.	100	17.9 mo.
EEG				
PSWCs	−		100	
CSF				
Positive 14-3-3 protein	+		88	
Pathology				
Plaque-like deposits of PrP	+		0	

dCJD = dura mater graft-associated Creutzfeldt–Jakob disease; PSWCs = periodic sharp-wave complexes; PrP = prion protein; yrs. = years; y/o = years old; mo. = months. The data on non-plaque type of dCJD are excerpts from reference [10].

Acknowledgments

The authors thank Prof. K. Doh-ura, Division of Prion Protein Biology, Department of Prion Research, Center for Translational and Advanced Animal Research on Human Diseases, Tohoku University Graduate School of Medicine, for measuring the level of 14-3-3 protein in the CSF.

References

[1] Parchi P, Giese A, Capellari S, Brown P, Schulz-Schaeffer W, Windl O, et al. Classification of sporadic Creutzfeldt–Jakob disease based on molecular and phenotypic analysis of 300 subjects. Ann Neurol 1999;46:224–33.
[2] Mead S, Stumpf MP, Whitfield J, Beck JA, Poulter M, Campbell T, et al. Balancing selection at the prion protein gene consistent with prehistoric kurulike epidemics. Science 2003;300:640–3.
[3] Shibuya S, Higuchi J, Shin RW, Tateishi J, Kitamoto T. Codon 219 Lys allele of PRNP is not found in sporadic Creutzfeldt–Jakob disease. Ann Neurol 1998;43:826–8.
[4] Tanaka Y, Minematsu K, Moriyasu H, Yamaguchi T, Yutani C, Kitamoto T, et al. A Japanese family with a variant of Gerstmann–Straussler–Scheinker disease. J Neurol Neurosurg Psychiatry 1997;62:454–7.
[5] Seno H, Tashiro H, Ishino H, Inagaki T, Nagasaki M, Morikawa S. New haplotype of familial Creutzfeldt–Jakob disease with a codon 200 mutation and a codon 219 polymorphism of the prion protein gene in a Japanese family. Acta Neuropathol 2000;99:125–30.
[6] Nishida Y, Sodeyama N, Toru Y, Toru S, Kitamoto T, Mizusawa H. Creutzfeldt–Jakob disease with a novel insertion and codon 219 Lys/Lys polymorphism in PRNP. Neurology 2004;63:1978–9.
[7] Hoshi K, Yoshino H, Urata J, Nakamura Y, Yanagawa H, Sato T. Creutzfeldt–Jakob disease associated with cadaveric dura mater grafts in Japan. Neurology 2000;55:718–21.
[8] Kaneko K, Zulianello L, Scott M, Cooper CM, Wallace AC, James TL, et al. Evidence for protein X binding to a discontinuous epitope on the cellular prion protein during scrapie prion propagation. Proc Natl Acad Sci USA 1997;94:10069–74.
[9] Hizume M, Kobayashi A, Teruya K, Ohashi H, Ironside JW, Mohri S, et al. Human prion protein (PrP) 219K is converted to PrPSc but shows heterozygous inhibition in variant Creutzfeldt–Jakob disease infection. J Biol Chem 2009;284:3603–9.
[10] Noguchi-Shinohara M, Hamaguchi T, Kitamoto T, Sato T, Nakamura Y, Mizusawa H, et al. Clinical features and diagnosis of dura mater graft-associated Creutzfeldt–Jakob disease. Neurology 2007;69:360–7.
[11] Kobayashi A, Asano M, Mohri S, Kitamoto T. Cross-sequence transmission of sporadic Creutzfeldt–Jakob disease creates a new prion strain. J Biol Chem 2007;282:30022–8.

Clinical Nephrology, Vol. 72 – No. 3/2009 (211-215)

clinical nephrology
Case Report

ISSN 0301-0430

Acute on chronic subdural hematoma as a rare complication in a microscopic polyangiitis patient receiving antithrombotic treatment

N. Takahashi[1], H. Kimura[1], R. Kitai[2], M. Sato[3], M. Yoneda[3], C. Yamamoto[1], D. Mikami[1], M. Kuriyama[3], T. Kubota[2], H. Itoh[4] and H. Yoshida[1]

[1]Department of General Medicine, Division of Nephrology, School of Medicine, Faculty of Medical Sciences, [2]Department of Sensory and Locomotor Medicine, Division of Neurosurgery, [3]Second Department of Internal Medicine (Neurology), and [4]Department of Pathological Sciences, Division of Tumor Pathology, School of Medicine, Faculty of Medical Sciences, University of Fukui, Japan

Key words
antithrombotic agent – membranous nephropathy (MN) – microscopic polyangiitis (MPA) – subdural hematoma (SDH)

Abstract. We report a 56-year-old man with microscopic polyangiitis (MPA) who developed acute exacerbation of a chronic subdural hematoma (SDH). Laboratory data demonstrated elevation of myeloperoxidase antineutrophil cytoplasmic antibody (MPO-ANCA) and rapidly progressing renal dysfunction. Renal biopsy showed crescentic glomerulonephritis (GN) with membranous nephropathy (MN). He was treated with corticosteroids, antithrombotic agents, and an immunosuppressant. One month after initiation of treatment, he had a mild headache. One month later, he developed acute SDH. Although he recovered completely after the operation, he finally died of bacterial infection. On autopsy, a scar of vasculitis was confirmed in the leptomeninges as well as in the kidney and lung. Although SDH is a rare complication in MPA, nephrologists must pay more attention to the initial symptoms before a hematoma attack such as headache, especially in patients using antithrombotic agents.

Received
August 7, 2008;
accepted in revised form
December 8, 2008

Correspondence and offprint requests to
H. Yoshida, MD, PhD, Professor
Division of Nephrology, Department of General Medicine, School of Medicine, Faculty of Medical Sciences, University of Fukui, Fukui, 910-1193, Japan
hayoshi@u-fukui.ac.jp

Introduction

Microscopic polyangiitis (MPA) is a vasculitis of the small-sized vessels that causes injury of various organs including kidney, lung, skeletal muscles, gastrointestinal tracts, skin and peripheral nerves [Jennette and Falk 1997].

In MPA, the involvement of the central nervous system (CNS) such as pachymeningitis or intracerebral hemorrhage occasionally observed in Wegener's granulomatosis [Nagashima et al. 2000] is rare, despite vasculitis of the similar sized vessels. Furthermore, subdural hematoma (SDH) is a very rare CNS involvement in MPA. Here, we report the first case that developed acute exacerbation of a chronic subdural hematoma (SDH) in the clinical course of MPA under antithrombotic treatment.

Case

A 56-year-old man was referred to our hospital with body weight loss and renal dysfunction on September 9, 2005. He had worked in Thailand as a technical expert. In 2002, his proteinuria was discovered for the first time, and his proteinuria gradually progressed. Since June 2005 he had lost weight (–7 kg in 3 months) and developed fever, cough and malaise. Although he had macrohematuria and edema in August, he had no headache, joint pain or myalgia. He came back to Japan and consulted a physician. He had severe proteinuria (> 300 mg/dl), hematuria (> 100 cells/high power field), and was suspected of rapidly progressive renal insufficiency (serum creatinine and blood urea nitrogen were 2.6 and 45.3 mg/dl, respectively).

On admission, he was 175 cm tall and weighed 60.5 kg. Blood pressure was 140/84 mmHg, pulse rate was 80/min regular, and body temperature was 36.9 °C. His conjunctiva was not anemic. Chest examination showed no murmur and no crackle. He had pitting edema of the lower extremities. There were no abnormal pigmentation, cyanosis or lymphnode swelling. Neurological examina-

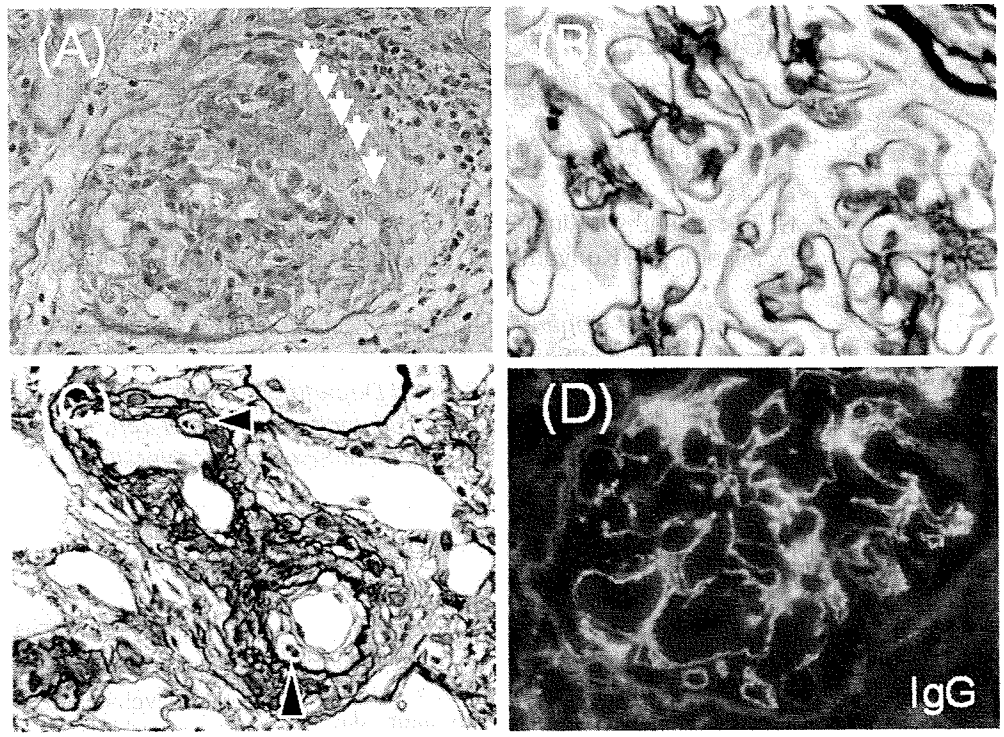

Figure 1. A: Light micrograph showing cellular crescent formation (arrows) in glomeruli (PAS, magnification × 400), B: no spike formation in GBM (PAM, magnification × 1,000), and C: mild hyalinosis in arterioles with mononuclear cell infiltration (arrowheads) (PAM, magnification × 400). D: Immunofluorescence micrograph showing granular IgG deposition along GBM.

tions showed no abnormalities. He had no habit of cocaine abuse.

Hematological tests revealed moderate leukocytosis. Chemistry data showed serum creatinine of 3.1 mg/dl, blood urea nitrogen 56 mg/dl, serum total protein 6.3 g/dl, serum albumin 3.4 g/dl total cholesterol 344 mg/dl. An immunological test showed a high titer of MPO-ANCA (> 640 EU). However, PR3-ANCA, antiglomerular basement membrane (GBM) antibody, antinuclear antibodies, antistreptolysin O, cryoglobulin, M-protein and complement fraction were all within normal limits or negative. Hepatitis B and C serology were negative. Urinalysis revealed 3+ protein with sediment findings of abundant deformed erythrocytes and pathological casts. The amount of 24-h urinary protein was 5.6 g/day, the urinary protein selectivity index was 0.18 indicating low selectivity proteinuria. Chest X-ray showed no cardiomegaly, pleural effusion or pneumonitis.

On September 14, a renal biopsy examined by light microscopy yielded 3 normal glomeruli, 4 sclerotic glomeruli and 6 glomeruli with cellular (Figure 1A) or fibro-cellular crescent formation. The GBM thickening or spike formation was not seen (Figure 1B). A wide area of tubular atrophy was observed. There were many mononuclear cells and fibrosis in the interstitium. Arterioles showed mild hyalinosis with mononuclear cell infiltration (Figure 1C). Immunofluorescence microscopy disclosed granular IgG staining (Figure 1D) and C3 staining along GBM. Since electron microscopy disclosed only sclerotic glomeruli, precise information of the thickness and dense depositions of GBM were not obtained.

According to these findings, necrotizing GN due to MPO-ANCA associated vasculitis with MN was diagnosed.

Clinical course

As the first-line treatment for necrotizing GN he was treated with 3 consecutive daily venous administrations of 1 g methylprednisolone and subsequent daily oral administration of 40 mg prednisolone (Figure 2). After angiotensin II antagonists were started, his blood pressure was sufficiently controlled. Furthermore, on September 20, classical hep-

arin treatment [Brown et al. 1974] for prevention of intraglomerular hypercoagulation due to necrotizing GN was started with cutaneous injection and the titration of the dose was done by checking the value of activated partial thromboplastin time (aPTT). The levels of proteinuria and MPO-ANCA titers gradually decreased and oral prednisolone was tapered. Despite the continuous decrease of MPO-ANCA titers, the daily amounts of urinary protein increased again. Thus, cyclosporine was coadministered since the worsened proteinuria was considered to be due to aggravation of coincident MN. After this, proteinuria began to decrease again (Figure 2).

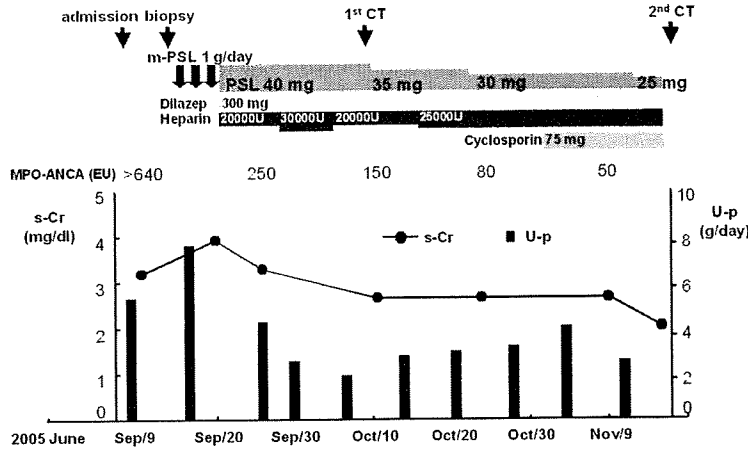

Figure 2. Clinical course of the patient. m-PSL, methylprednisolone, PSL, prednisolone.

On October 1, he had a mild headache for the first time since before admission. Head-computed tomography (CT) was performed for the first time on October 3 and was considered to be within normal limits by a radiologist (Figure 3A). We did not think that cranial magnetic resonance images (MRI) were necessary for this patient at that time. However, he was later diagnosed with chronic SDH by a neurosurgeon. On the morning of November 13, he suddenly had a strong headache and rapidly developed a coma. Head CT revealed a medium-sized high-density area with midline shift, indicating acute SDH (Figure 3B), and no skull fracture. He finally underwent decompression craniectomy. A fibrosing capsule as in pachymeningitis was observed over leptomeninges around the SDH, but no remarkable dural thickening was observed. The drainage fluid after craniectomy was not pus-like but simply sanguineous as described previously [Yokote et al. 1997]. Although he recovered completely from the impaired consciousness, he finally died of bacterial infection 8 months after the operation.

On autopsy, brain tissue was obtained and scarring of vasculitis in the leptomeninges was observed (Figure 4A,B) as well as in the kidney and lung (Figure 4C). However, there were no findings of any other causes of SDH such as aneurysm in the subarachnoidea, arteriovenous malformation, meningioma or dural cancer metastasis.

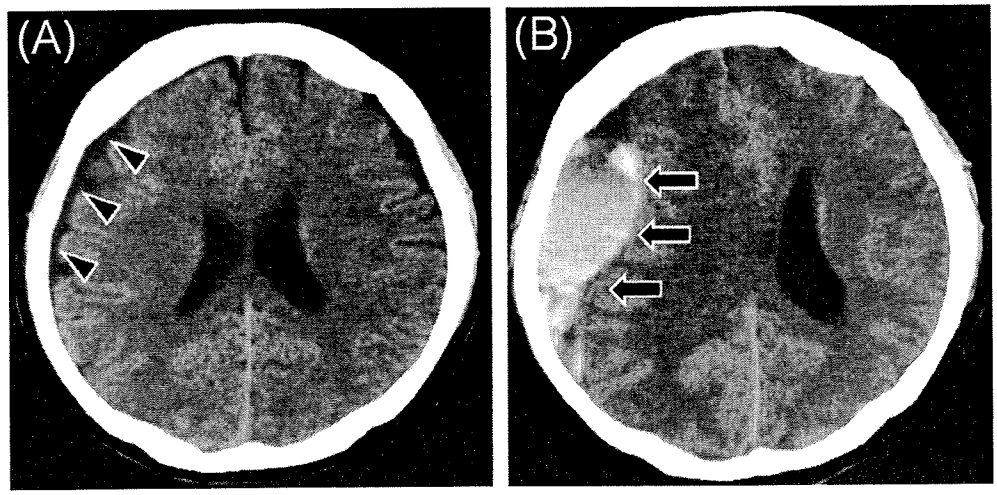

Figure 3. A: Axial computed tomographic scan of the head indicating chronic SDH shown as iso-density area in the right temporal lobe on October 3 (arrowheads), B: acute SDH shown as high-density area in the right temporal lobe on November 13 (arrows).

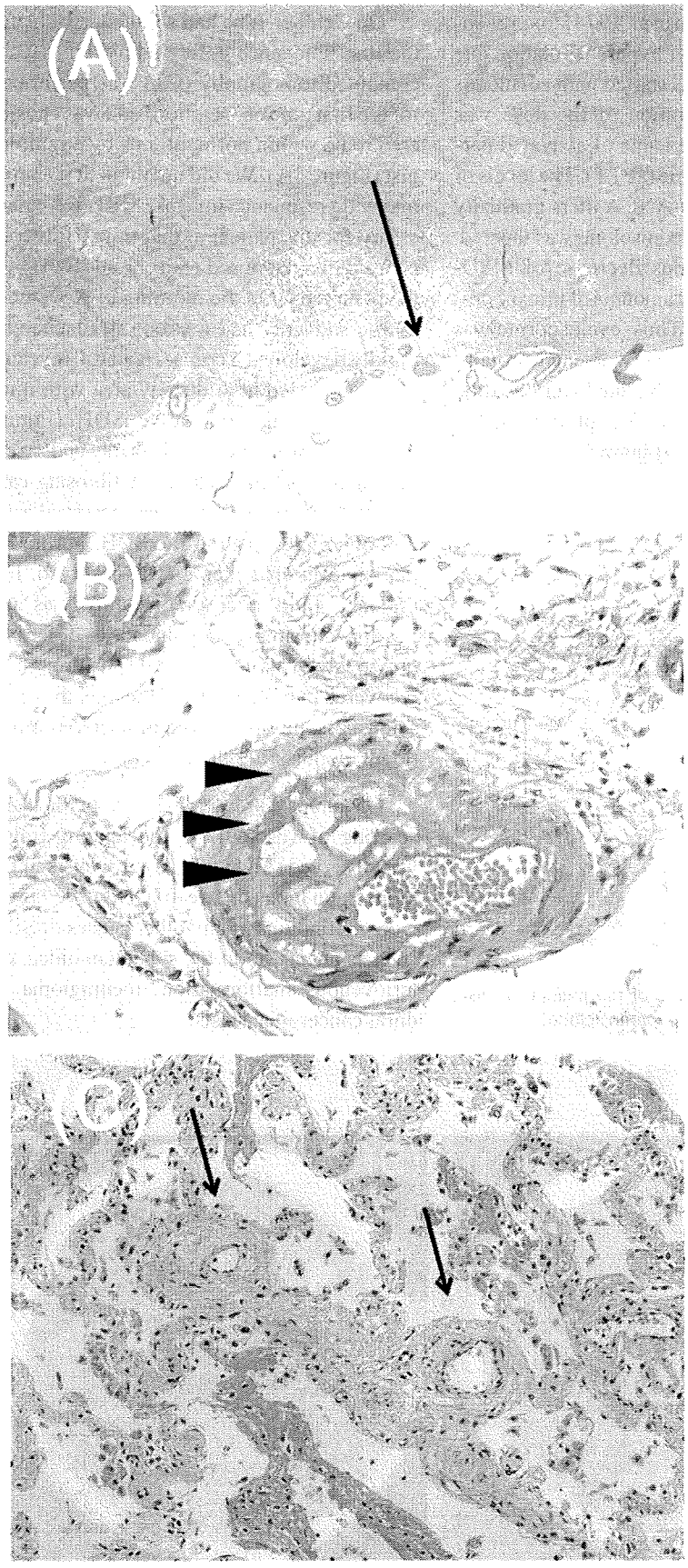

Figure 4. A,B: The scar of vasculitis in leptomeninges. HE, magnification × 40, × 400, respectively), C: The scar of vasculitis in lung (HE, magnification × 200).

Discussion

Vasculitis is classified according to the size and distribution of inflamed vessels [Jennette et al. 1994]. In this case, the inflammation in the small vessels of the kidney and lung was confirmed on autopsy. Then, he was finally diagnosed with MPA rather than MPO-ANCA associated necrotizing GN. Furthermore, scarring of vasculitis was confirmed in the leptomeninges of autopsy tissues. Interestingly, this finding suggests that fragility of the vessels damaged by inflammation insult could be a partial cause of this SDH.

In MPA, peripheral nervous system involvement commonly occurs [Jennette and Falk 1997], while CNS involvement has rarely been reported. There were only a few reported cases that were complicated with pachymeningitis [Jacobi et al. 2005, Kono et al. 2000, Saeki et al. 2004, Takahashi et al. 1998], optic neuropathy [Harada et al. 1997], multiple cranial neuropathies [Morinaga et al. 2007], reversible posterior leukoencephalopathy [Tajima and Matsumoto, 2006], or intracerebral hemorrhage [Ito et al. 2006] in p-ANCA or MPO-ANCA positive patients. To our knowledge, this case is the first report for SDH occurrence with CNS involvement associated with MPA.

Song et al. [2005] reported a polyarteritis nodosa patient with acute pachymeningitis with non-contrast CT images mimicking subdural hematoma. They confirmed the pachymeningitis with contrast-enhanced MRI. We could not directly find remarkable inflamed thickening of the dura at his craniectomy, nor had we any time to perform MRI before the urgent operation. Therefore, we could not exclude completely the possibility of subclinical or mild pachymeningitis.

In general, common causes of SDH are trauma and the use of antithrombotic agents [So et al. 1983]. Rare causes are subarachnoid aneurysm, arteriovenous malformation, meningioma, dural cancer metastasis, complication of systemic thrombolytic therapy for acute myocardial infarction, cerebrospinal fluid hypotension and cocaine abuse. Although head trauma is the most common cause to be considered, he had no history of trauma before and after his admission.

As for antithrombotic treatment, he certainly received both heparin and an anti-

platelet agent for the treatment of necrotizing GN and MN. In fact, Raymond et al. [1992] reported that the use of antithrombotic agents could increase the independent risk of chronic SDH in patients with head trauma. Although the values of aPTT were within therapeutic ranges during the treatment in this case, we should have been more cautious with the administration of antithrombotic agents.

In contrast, Gore et al. [1991] reported that only 0.1 – 0.2% of patients with myocardial infarction had SDH complications during treatment with heparin, aspirin and intravenous recombinant tissue-type plasminogen activator. Therefore, if vessels had no injury with vasculitis, the frequency of SDH during the treatment with plural antithrombotic agents should be extremely rare.

Since in autopsy specimens of the brain, inflammatory scars of small vessels in leptomeninges were confirmed, we assume that ANCA-associated vasculitis had subclinically developed in small vessels of the brain surface in the earlier stage and that resulted in fragility of vessel walls, which predisposed this patient to SDH. Hence, it is reasonable to conclude that the cause of SDH in this case was due to combined factors (both vasculitis and the subsequent use of antithrombotic agents) rather than one factor (either vasculitis or the use of antithrombotic agents).

Finally, since nephrologists frequently treat MPA with antithrombotic agents, we should be more cautious and consider mild headaches as the possible initial symptom of SDH, which is a very rare but serious CNS complication of MPA.

Acknowledgments

We sincerely thank Mr. Maegawa, Mr. Mori and Mr. Kato for valuable technical assistance.

References

Brown CB, Wilson D, Turner D, Cameron JS, Ogg CS, Chantler C, Gill D. Combined immunosuppression and anticoagulation in rapidly progressive glomerulonephritis. Lancet. 1974; *2:* 1166-1172.

Gore JM, Sloan M, Price TR, Randall AM, Bovill E, Collen D, Forman S, Knatterud GL, Sopko G, Terrin ML. Intracerebral hemorrhage, cerebral infarction, and subdural hematoma after acute myocardial infarction and thrombolytic therapy in the thrombolysis in myocardial infarction study. Thrombolysis in myocardial infarction, Phase II, pilot and clinical trial. Circulation. 1991; *83:* 448-459.

Harada T, Ohashi T, Harada C, Yoshida K, Maguchi S, Moriwaka F, Matsuda H. A case of bilateral optic neuropathy and recurrent transverse myelopathy associated with perinuclear antineutrophil cytoplasmic antibodies (P-ANCA). J Neuroophthalmol. 1997; *17:* 254-256.

Ito Y, Suzuki K, Yamazaki T, Yoshizawa T, Ohkoshi N, Matsumura A. ANCA-associated vasculitis (AAV) causing bilateral cerebral infarction and subsequent intracerebral hemorrhage without renal and respiratory dysfunction. J Neurol Sci. 2006; *240:* 99-101.

Jacobi D, Maillot F, Hommet C, Arsene S, Cottier JP, Lamisse F, Guillevin L. P-ANCA cranial pachymeningitis: a case report. Clin Rheumatol. 2005; *24:* 174-177.

Jennette JC, Falk RJ. Small-vessel vasculitis. N Engl J Med. 1997; *337:* 1512-1523.

Jennette JC, Falk RJ, Andrassy K, Bacon PA, Churg J, Gross WL, Hagen EC, Hoffman GS, Hunder GG, Kallenberg CG et al. Nomenclature of systemic vasculitides. Proposal of an international consensus conference. Arthritis Rheum. 1994; *37:* 187-192.

Kono H, Inokuma S, Nakayama H, Yamazaki J. Pachymeningitis in microscopic polyangiitis (MPA). A case report and a review of central nervous system involvement in MPA. Clin Exp Rheumatol. 2000; *18:* 397-400.

Morinaga A, Ono K, Komai K, Yamada M. Microscopic polyangitis presenting with temporal arteritis and multiple cranial neuropathies. J Neurol Sci. 2007; *256:* 81-83.

Nagashima T, Maguchi S, Terayama Y, Horimoto M, Nemoto M, Nunomura M, Mori M, Seki T, Matsukawa S, Itoh T, Nagashima K. P-ANCA-positive Wegener's granulomatosis presenting with hypertrophic pachymeningitis and multiple cranial neuropathies: Case report and review of literature. Neuropathology. 2000; *20:* 23-30.

Reymond MA, Marbet G, Radu EW, Gratzl O. Aspirin as a risk factor for hemorrhage in patients with head injuries. Neurosurg Rev. 1992; *15:* 21-25.

Saeki T, Fujita N, Kourakata H, Yamazaki H, Miyamura S. Two cases of hypertrophic pachymeningitis associated with myeloperoxidase antineutrophil cytoplasmic autoantibody (MPO-ANCA)-positive pulmonary silicosis in tunnel workers. Clin Rheumatol. 2004; *23:* 76-80.

So W, Hugenholtz H, Richard MT. Complications of anticoagulant therapy in patients with known central nervous system lesions. Can J Surg. 1983; *26:* 181-183.

Song JS, Lim MK, Park BH, Park W. Acute pachymeningitis mimicking subdural hematoma in a patient with polyarteritis nodosa. Rheumatol Int. 2005; *25:* 637-640.

Tajima Y, Matsumoto A. Reversible posterior leukoencephalopathy syndrome in P-ANCA-associated vasculitis. Intern Med. 2006; *45:* 1169-1171.

Takahashi K, Kobayashi S, Okada K, Yamaguchi S. Pachymeningitis with a perinuclear antineutrophil cytoplasmic antibody: response to pulse steroid. Neurology. 1998; *50:* 1190-1191.

Yokote H, Terada T, Nakai K, Itakura T. Subdural and meaningful involvement related to Wegener's granulomatosis: Case report. Neurosurgery. 1997; *40:* 1071-1074.